DAVID W. TAYLOR NAVAL SHIP RESEARCH AND DEVELOPMENT CENTER

Bethesda, Maryland 20084

SAD-84/1E-1902

TURBULENT BOUNDARY LAYER BENEATH BLANKETS:
MEASUREMENTS AND INTERPRETATIONS

by

F.E. Geib and G. Maidanik

Approved for public release;
distribution unlimited.

SHIP ACOUSTICS DEPARTMENT
DEPARTMENTAL REPORT

SAD-84/1E-1902

October 1983

TURBULENT BOUNDARY LAYER BENEATH BLANKETS:
MEASUREMENTS AND INTERPRETATIONS

MAJOR DTNSRDC ORGANIZATIONAL COMPONENTS

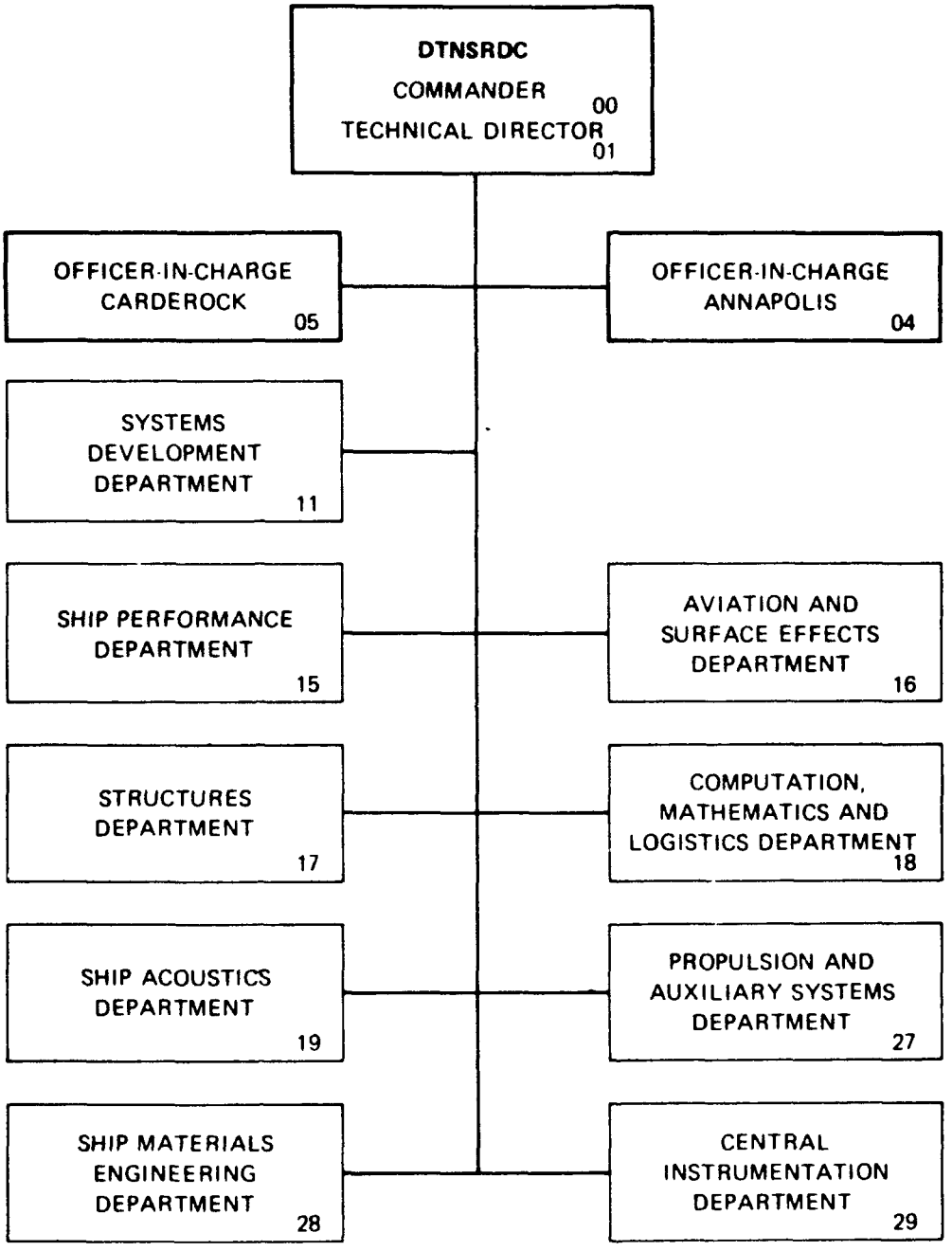

DEPARTMENT OF THE NAVY

DAVID W. TAYLOR
NAVAL SHIP RESEARCH AND DEVELOPMENT CENTER
BETHESDA, MD 20084

TURBULENT BOUNDARY LAYER BENEATH BLANKETS:

MEASUREMENTS AND INTERPRETATIONS

by

F.E. Geib and G. Maidanik

Approved for public release;
distribution unlimited.

October 1983

SAD-84/1E-1902

TABLE OF CONTENTS

LIST OF FIGURES

LIST OF FIGURES (continued)

ABSTRACT

An analytical estimate of the performance of a blanket as a spatial-temporal filter for turbulent boundary layer pressure fluctuations is presented. The formulation is developed as an aid for the design of experiments and experimental procedures for measuring the performance of blankets. The interpretation of data acquired in such experiments is treated in some detail. A simplified analytical model is utilized which has the gross features of the pressure field beneath a convecting turbulent boundary layer. This serves to illustrate the trends that can be anticipated in data and to illustrate the effects of undesirable stray pressure fields. Some limited data were acquired in a quiet turbulent pipe facility and are treated with the developed formalism. Significant features in the data are briefly discussed.

ADMINISTRATIVE INFORMATION

The work described in this report was funded under the David Taylor Naval Ship Research and Development Center's Independent Research Program, Program Element 61152N, Task Area ZR 011 0801, Work Units 1902-025, 1902-027, and 1942-053.

I. INTRODUCTION

The movement of vehicles through fluid media usually causes the fluid to become unstable at various locations on the outer plating of the vehicles. Indeed, over extended regions of the outer plating, a turbulent boundary layer is formed. The fluctuations that are present in the flow of a turbulent boundary layer induce pressure fields on the surfaces on which they form; these pressure fields exhibit both spatial and temporal variations. The pressure fields that are induced by turbulent boundary layers constitute drives that generate acoustic noise, be it in the form of radiation noise to the far field or in the form of local noise in the interior and on the vehicle. Often, at the higher operational speeds of these vehicles the noises that are flow-induced are significant and well-nigh dominant. Amongst them is the noise that is generated by a turbulent boundary layer. The suppression of these noises has been central to many noise control programs. Progress has been made, but

no means has it been sufficient. The progress is manifested in understanding ith the generating mechanism and the nature of the pressure fields in turbulent undary layers, as well as in devising means to control or suppress their adverse fects. In this paper, the authors report a small but significant step in the fort to control or reduce the noises that a turbulent boundary layer may generate. device that appears to have promise of beneficially controlling and reducing the essure field exerted on a surface by a turbulent boundary layer is a blanket. An ieally designed blanket is a device hat displaces the turbulent boundary layer a lanket thickness away from the surface on which it would have formed were the lanket absent. To state the function of a blanket more precisely it may be advantageous to formulate its use. However, it may be useful to gear the formalism so hat it may also be employed to examine and interpret data yielded by a recent xperiment. In this experiment, the output of an array of flush-mounted pressure ransducers subject to the pressure field in a turbulent boundary layer was investiated. The array was constructed and used, for the most part, as a wavevector filer [1]. The influence of interjecting a blanket between the pressure field and the rray was of particular interest in this experiment.

II. OUTPUTS OF AN ARRAY OF FLUSH-MOUNTED PRESSURE TRANSDUCERS PLACED ON A UNIFORM PLANE BOUNDARY

Consider a plane boundary in which are placed flush-mounted pressure transucers. The transducers are placed so that their presence introduces no impedance onuniformities in the boundary so that the surface impedance operator $z^b(\underset{\sim}{x},t)$ of he plane boundary is pure; $\underset{\sim}{x} = \{x_1,x_2\}$ is the spatial vector coordinate in the lane and t is the temporal coordinate [2]. Ignoring effects of the steady flow and oncentrating only on the fluctuating components, the pressure field $p(\underset{\sim}{x},t)$ on the oundary can be expressed in the form

$$p(\underset{\sim}{x},t) = z^b(\underset{\sim}{x},t)\, v(\underset{\sim}{x},t) = 2p_e^{\nu}(\underset{\sim}{x},t) - p^{\nu}(\underset{\sim}{x},t), \tag{1}$$

where $p_e^{\nu}(\underset{\sim}{x},t)$ and $p^{\nu}(\underset{\sim}{x},t)$ are the incident test external pressure field drive and the fluid loading on the plane, respectively, and $v(\underset{\sim}{x},t)$ is the velocity field on the boundary induced by the incident test external drive. In spectral space, Equation (1) can be cast in the form [2]

$$P(\underset{\sim}{k},\omega) = Z^b(\underset{\sim}{k},\omega)\, V(\underset{\sim}{k},\omega) = 2P_e^{\nu}(\underset{\sim}{k},\omega) - P^{\nu}(\underset{\sim}{k},\omega)\ , \tag{2}$$

where

$$P^{\nu}(\underset{\sim}{k},\omega) = Z^{\nu}(\underset{\sim}{k},\omega)\, V(\underset{\sim}{k},\omega) \quad ; \tag{3a}$$

$$Z^{\nu}(\underset{\sim}{k},\omega) = (\rho_{\nu} c_{\nu}/\kappa_3^{\nu}) \ ; \tag{3b}$$

$$\kappa_3^{\nu} = [1-(\kappa^{\nu})^2]^{1/2}\, U[1-(\kappa^{\nu})^2] - i[(\kappa^{\nu})^2-1]\, U[(\kappa^{\nu})^2 -1] \ ; \tag{3c}$$

the Fourier transform is defined by

$$S(\underset{\sim}{k},\omega) = (2\pi)^{-3/2} \int d\underset{\sim}{x} \int dt\ s(\underset{\sim}{x},t)\, \exp[i(\underset{\sim}{k}\cdot\underset{\sim}{x}-\omega t)]; \tag{4a}$$

$$d\underset{\sim}{x} = dx_1\, dx_2 \ ; \ \underset{\sim}{k} = \{k_1,k_2\} \quad ; \quad k = |\underset{\sim}{k}| \ ; \tag{4b}$$

$\underset{\sim}{\kappa}^{\nu}$ is a normalized wavevector

$$\underset{\sim}{\kappa}^{\nu} = \{\kappa_1^{\nu},\kappa_2^{\nu}\} \ ; \ \kappa^{\nu} = |\underset{\sim}{\kappa}^{\nu}| \ ; \ \kappa_i^{\nu} = (\kappa_i c_{\nu}/\omega) \ ; \tag{4c}$$

the density ρ_{ν} and speed of sound c_{ν} are those of the semi-infinite fluid occupying the space above the boundary, see Figure 1; the purity of the surface impedance

operator $z^b(\underset{\sim}{x},t)$ is invoked; $s(\underset{\sim}{x},t)$ in Equation (4) is any typical well-behaved function of $\underset{\sim}{x}$ and t; and U is the step function. From Equation (2), one obtains

$$V(\underset{\sim}{k},\omega) = [Z^b(\underset{\sim}{k},\omega) + Z^\nu(\underset{\sim}{k},\omega)]^{-1}\ 2P_e^\nu(\underset{\sim}{k},\omega)\ , \tag{5}$$

$$P(\underset{\sim}{k},\omega) = [1+T^b_{\nu\nu}(\underset{\sim}{k},\omega)]\ P_e^\nu(\underset{\sim}{k},\omega)\ , \tag{6}$$

$$(1/2)[1+T^b_{\nu\nu}(\underset{\sim}{k},\omega)] = Z^b(\underset{\sim}{k},\omega)\ [Z^b(\underset{\sim}{k},\omega) + Z^\nu(\underset{\sim}{k},\omega)]^{-1}\ , \tag{7}$$

where the quantity $T^b_{\nu\nu}(\underset{\sim}{k},\omega)$ can be identified to be the reflection coefficient at the boundary facing the (ν)-fluid.

The pressure $p(\underset{\sim}{x},t)$ on the boundary is sensed by the flush-mounted pressure transducers. This array of transducers is assumed to possess a filtering function $g'(\underset{\sim}{x}_o|\underset{\sim}{x},t_o|t)$ so that the output $q(\underset{\sim}{x}_o,t_o)$ is given by

$$q(\underset{\sim}{x}_o,t_o) = \int d\underset{\sim}{x} \int dt\ g'(\underset{\sim}{x}_o|\underset{\sim}{x},t_o|t)\ p(\underset{\sim}{x},t)\ . \tag{8}$$

The spatial-temporal vector $\{\underset{\sim}{x}_o,t_o\}$ defines a specific spatial-temporal positioning of the array. Using Equation (4), Equation (8) can be cast in spectral space in the form

$$Q(\underset{\sim}{k},\omega) = \int d\underset{\sim}{k}' \int d\omega'\ G'(\underset{\sim}{k}|\underset{\sim}{k}',\omega|\omega')\ P(\underset{\sim}{k}',\omega')\ , \tag{9}$$

where

$$q(\underset{\sim}{x}_o,t_o) = (2\pi)^{-3/2} \int d\underset{\sim}{k} \int d\omega\ Q(\underset{\sim}{k},\omega)\ \exp[-i(\underset{\sim}{k}\cdot\underset{\sim}{x}_o-\omega t_o)];$$

$$Q(\underset{\sim}{k},\omega) = (2\pi)^{-3/2} \int d\underset{\sim}{x}_o \int dt_o q(\underset{\sim}{x}_o,t_o)\ \exp[i(\underset{\sim}{k}\cdot\underset{\sim}{x}_o+\omega t_o)]\ , \tag{10}$$

$$g'(\underset{\sim}{x}_o|\underset{\sim}{x},t_o|t) =$$

$$(2\pi)^{-3} \int d\underset{\sim}{k} \int d\omega \int d\underset{\sim}{k}' \int d\omega' \; G'(\underset{\sim}{k}|\underset{\sim}{k}'\omega|\omega') \exp[-i(\underset{\sim}{k}\cdot\underset{\sim}{x}_o - \underset{\sim}{k}'\cdot\underset{\sim}{x} - \omega t_o + \omega' t)];$$

$$G'(\underset{\sim}{k}|\underset{\sim}{k}'\omega|\omega') =$$

$$(2\pi)^{-3} \int d\underset{\sim}{x}_o \int dt_o \int d\underset{\sim}{x} \int dt \; g'(\underset{\sim}{x}_o|\underset{\sim}{x},t_o|t) \exp[i(\underset{\sim}{k}\cdot\underset{\sim}{x}_o - k'\cdot\underset{\sim}{x} - \omega t_o + \omega' t)] \; . \qquad (11)$$

It is now assumed that the filtering function $g'(\underset{\sim}{x}_o|\underset{\sim}{x},t_o|t)$ is stationary, both spatially and temporally, so that

$$g'(\underset{\sim}{x}_o|\underset{\sim}{x},t_o|t) \equiv (2\pi)^{-3/2} \; g(\underset{\sim}{x}_o - \underset{\sim}{x}, t_o - t) \; . \qquad (12)$$

In spectral space, Equation (12) takes the form

$$G'(\underset{\sim}{k}|\underset{\sim}{k}',\omega|\omega') \equiv G(\underset{\sim}{k},\omega) \; \delta(\underset{\sim}{k}-\underset{\sim}{k}') \; \delta(\omega-\omega') \qquad (13)$$

$$\delta(\underset{\sim}{k}-\underset{\sim}{k}') = \delta(k_1 - k_1') \; \delta(k_2 - k_2') \qquad (14)$$

Substituting Equation (13) in Equation (9), one obtains

$$Q(\underset{\sim}{k},\omega) = G(\underset{\sim}{k},\omega) \; P(\underset{\sim}{k},\omega) \; . \qquad (15)$$

Usually, and quite generally, the vector $\{\underset{\sim}{x}_o, t_o\}$ is set identically equal to zero so that from Equations (6), (10), and (15), one obtains

$$q(0,0) = q = \int d\underset{\sim}{k} \int d\omega \; G(\underset{\sim}{k},\omega) \; P(\underset{\sim}{k},\omega) \quad , \qquad (16a)$$

$$q = \int d\underset{\sim}{k} \int d\omega \; \{G(\underset{\sim}{k},\omega) \; [1+T^{b}_{\nu\nu}(\underset{\sim}{k},\omega)]\} \; P^{\nu}_{e}(\underset{\sim}{k},\omega) \; . \tag{16b}$$

Thus, with reference to the indigenous drive $P(\underset{\sim}{k},\omega)$, the filtering function of the flush-mounted array is $G(\underset{\sim}{k},\omega)$. On the other hand, with reference to the incident test external drive $P^{\nu}_{e}(\underset{\sim}{k},\omega)$, the filtering function of the flush-mounted array is $\{G(\underset{\sim}{k},\omega) \; [1+T^{b}_{\nu\nu}(\underset{\sim}{k},\omega)]\}$. Of course, the particular designation of the drives and the corresponding filtering functions is a matter of convenience and interpretation; the integrands are, after all, the same in these cases and, therefore, the outputs are also the same. Having determined the output of the array in the absence of a blanket, attention is turned to determining the central question posed in this paper. How does a blanket placed on the flush-mounted array just considered influence the output of the array?

III. INFLUENCE OF A BLANKET ON THE OUTPUT OF A FLUSH-MOUNTED ARRAY

The introduction of the blanket is depicted in Figure 2. The blanket is featured here as a slab of fluid of density ρ_{ℓ}, speed of sound c_{ℓ}, and width h_{ℓ}. The bottom side of the blanket is backed by the boundary previously discussed. In this boundary is placed the flush-mounted array. The top side of the blanket is backed by a semi-infinite space occupied by the (ν)-fluid. The pressure field is considered to be generated by the incident test external drive $P^{\nu}_{e}(\underset{\sim}{k},\omega)$ which acts on the top surface of the blanket. The pressure field $P^{\nu}_{\ell}(\underset{\sim}{k},z,\omega)$ in the blanket at a plane a separation z above the boundary is composed of two components,

$$P_{\ell}(\underset{\sim}{k},z,\omega) = P_{\ell+}(\underset{\sim}{k},z,\omega) + P_{\ell-}(\underset{\sim}{k},z,\omega) \tag{17}$$

as indicated in Figure 2. The pressure field $P_{\ell+}$ propagates down toward the boundary and $P_{\ell-}$ propagates up away from the boundary. The derivation of the pressure fields $P_{\ell+}$ and $P_{\ell-}$ is greatly facilitated if it is conducted in spectral

space. It can be readily shown that [3]

$$P_{\ell+}(\underset{\sim}{k},\omega) = \exp(ik_\ell z)\ \bar{T}_{\ell\nu}(\underset{\sim}{k},\omega)$$

$$\times\ [1-\bar{T}^b_{\ell\ell}(\underset{\sim}{k},\omega)\ \bar{T}^\nu_{\ell\ell}(\underset{\sim}{k},\omega)]^{-1}\ P^\nu_e(\underset{\sim}{k},\omega)\ , \tag{18a}$$

$$P_{\ell-}(\underset{\sim}{k},\omega) = \bar{T}^b_{\ell\ell}\ \exp(-ik_\ell z)\ \bar{T}_{\ell\nu}(\underset{\sim}{k},\omega)$$

$$\times\ [1-\bar{T}^b_{\ell\ell}(\underset{\sim}{k},\omega)\ \bar{T}^\nu_{\ell\ell}(\underset{\sim}{k},\omega)]^{-1}\ P^\nu_e(\underset{\sim}{k},\omega)\ , \tag{18b}$$

where

$$(1/2)\ [1+T^\alpha_{\ell\ell}(\underset{\sim}{k},\omega)] = Z^\alpha(\underset{\sim}{k},\omega)\ [Z^\alpha(\underset{\sim}{k},\omega) + Z^\ell(\underset{\sim}{k},\omega)]^{-1}\ , \tag{19a}$$

$$(1/2)\ T_{\ell\nu}(\underset{\sim}{k},\omega) = Z^\ell(\underset{\sim}{k},\omega)\ [Z^\nu(\underset{\sim}{k},\omega) + Z^\ell(\underset{\sim}{k},\omega)]^{-1}\ , \tag{19b}$$

$$\bar{T}(\underset{\sim}{k},\omega) = \exp(-ik_\ell h_\ell)\ T(\underset{\sim}{k},\omega)\quad ;\quad k_\ell = (\omega/c_\ell)\ \kappa^\ell_3\ , \tag{19c}$$

$$\kappa^\ell_3 = [1-(\kappa^\ell)^2]^{1/2}\ U[1-(\kappa^\ell)^2]\ -i\,[(\kappa^\ell)^2-1]^{1/2}\ U[(\kappa^\ell)^2-1]\ . \tag{19d}$$

The pressure field $P_\ell(\underset{\sim}{k},o,\omega) = P_\ell(\underset{\sim}{k},\omega)$ on the boundary is given by

$$P_\ell(\underset{\sim}{k},\omega) = P_{\ell+}(\underset{\sim}{k},\omega) + P_{\ell-}(\underset{\sim}{k},\omega) = [1+T^b_{\ell\ell}(\underset{\sim}{k},\omega)]\ \bar{T}_{\ell\nu}(\underset{\sim}{k},\omega)$$

$$\times\quad [1-\bar{T}^b_{\ell\ell}(\underset{\sim}{k},\omega)\ \bar{T}^\nu_{\ell\ell}(\underset{\sim}{k},\omega)]^{-1}\ P^\nu_e(\underset{\sim}{k},\omega) \tag{20}$$

[Cf. Equation (6).] This is the indigerous pressure field that is sensed by the array. Following a procedure similar to that which led from Equation (8) to Equation (16), the output $q_\ell(h_\ell) = q_\ell$ of the blanketed array is given by

$$q_\ell = \int d\underset{\sim}{k} \int d\omega \; G(\underset{\sim}{k},\omega) \; P_\ell(\underset{\sim}{k},\omega) \quad , \tag{21a}$$

$$q_\ell = \int d\underset{\sim}{k} \int d\omega \; \{G(\underset{\sim}{k},\omega) \; [1+T^b_{\ell\ell}(\underset{\sim}{k},\omega)]\} \; \bar{T}_{\ell\nu}(\underset{\sim}{k},\omega)$$

$$\times \; [1-\bar{T}^b_{\ell\ell}(\underset{\sim}{k},\omega) \; \bar{T}^\nu_{\ell\ell}(\underset{\sim}{k},\omega)]^{-1} \; P^\nu_e(\underset{\sim}{k},\omega). \tag{21b}$$

A similar remark to that following Equation (16) can be made with respect to Equation (21). Finally, if the fluid of the blanket, the (ℓ)-fluid, is chosen to match that of the (ν)-fluid, Equation (21b) is substantially simplified and becomes

$$q^\nu_\ell = \int d\underset{\sim}{k} \int d\omega \; \{G(\underset{\sim}{k},\omega)[1+T^b_{\nu\nu}(\underset{\sim}{k},\omega)]\}\{\exp(-ik_\ell h_\ell)\} \; P^\nu_e(\underset{\sim}{k},\omega), \tag{21c}$$

where $\rho_\ell = \rho_\nu$ and $c_\ell = c_\nu$. Comparing Equation (16b) with Equations (21b) and (21c), one finds that the presence of the blanket is accounted for by introducing the factor

$$F_\ell(\underset{\sim}{k},\omega) = [1+T^b_{\ell\ell}(\underset{\sim}{k},\omega)][1+T^b_{\nu\nu}(\underset{\sim}{k},\omega)]^{-1}$$

$$\times \; \bar{T}_{\ell\nu}(\underset{\sim}{k},\omega) \; [1-\bar{T}^b_{\ell\ell}(\underset{\sim}{k},\omega) \; \bar{T}^\nu_{\ell\ell}(\underset{\sim}{k},\omega)]^{-1} \quad , \tag{22a}$$

$$F^\nu_\ell(\underset{\sim}{k},\omega) = \exp[-ik^\nu_j h^\nu_\ell] \; ; \quad h^\nu_\ell = (\omega h_\ell / c_\nu); \tag{22b}$$

if $\rho_\ell = \rho_\nu$ and $c_\ell = c_\nu$, in the integrand of the output of the array as stated in

Equation (16). Thus, if the filtering function $F(\underset{\sim}{k},\omega)$ in the absence of a blanket is defined by

$$F(\underset{\sim}{k},\omega) = F_a(\underset{\sim}{k},\omega)\, F_b(\underset{\sim}{k},\omega) \quad ; \quad F_a(\underset{\sim}{k},\omega) = G(\underset{\sim}{k},\omega) \quad ; \quad F_b(\underset{\sim}{k},\omega) = [1+T^b_{\nu\nu}(\underset{\sim}{k},\omega)], \tag{23}$$

then from Equations (16b) and (21b) through (23), one obtains

$$q = \int d\underset{\sim}{k} \int d\omega\; F(\underset{\sim}{k},\omega)\; P^{\nu}_e(\underset{\sim}{k},\omega) \quad , \tag{24a}$$

$$q_\ell(h_\ell) = \int d\underset{\sim}{k} \int d\omega\; F(\underset{\sim}{k},\omega)\; F_\ell(\underset{\sim}{k},\omega)\; P^{\nu}_e(\underset{\sim}{k},\omega) \quad , \tag{24b}$$

$$q^{\nu}_\ell(h_\ell) = \int d\underset{\sim}{k} \int d\omega\; F(\underset{\sim}{k},\omega)\; F^{\nu}_\ell(\underset{\sim}{k},\omega)\; P_e(\underset{\sim}{k},\omega) \quad . \tag{24c}$$

The quantities $F_a(\underset{\sim}{k},\omega)$, $F_b(\underset{\sim}{k},\omega)$, and $F_\ell(\underset{\sim}{k},\omega)$ may be dubbed the filtering functions of the array, the boundary, and the blanket, respectively. A blanket that can be made to possess a filtering function $F^{\nu}_\ell(\underset{\sim}{k},\omega)$, as stated in Equation (22b), is dubbed ideal.

IV. QUADRATIC AND STATISTICAL FORMS FOR THE PRESSURE FIELD ON A BOUNDARY

Consider the pressure field $p_b(\underset{\sim}{x},t)$ acting on a plane surface. There are situations in which the quadratic form of the pressure field is the desired description. This quadratic form is defined by

$$\Psi'_b(\underset{\sim}{x}|\underset{\sim}{x}',t|t') = [p_b(\underset{\sim}{x},t)\; p^*_b(\underset{\sim}{x}',t')] \quad . \tag{25}$$

This form is usually desired when the linear description is difficult so that a

statistical description is preferred. To indicate that appropriate statistical averaging has been performed, the quantity is enclosed in angular brackets so that

$$\psi_b(\underset{\sim}{x}|\underset{\sim}{x}',t|t') = \langle\psi_b'(\underset{\sim}{x}|\underset{\sim}{x}',t|t')\rangle = \langle p_b(\underset{\sim}{x},t)\ p_b^*(\underset{\sim}{x}',t')\rangle\ . \tag{26}$$

The desirability of casting the pressure field in its quadratic and statistical form is often dictated by the fact that pressure fields in this form can be assumed to be stationary, both spatially and temporally, so that

$$\psi_b(\underset{\sim}{x}|\underset{\sim}{x}',t|t') \equiv (2\pi)^{-3/2}\ \phi_b(\underset{\sim}{x}-\underset{\sim}{x}',t-t')\ . \tag{27}$$

This assumption is seldom strictly true in practice. Nevertheless, provided the phenomenon that is being formulated is not strongly dependent on the deviation of the quadratic and statistical form of the pressure field from stationarity, the assumption is tempting; the simplicity that is gained in the formalism makes it attractive. Converting Equations (25) through (27) into spectral space yields

$$\Psi_b'(\underset{\sim}{k}|\underset{\sim}{k}',\omega|\omega') = [P_b(\underset{\sim}{k},\omega)\ P_b^*(\underset{\sim}{k}',\omega')]\ , \tag{28}$$

$$\Psi_b(\underset{\sim}{k}|\underset{\sim}{k}',\omega|\omega') = \langle P_b(\underset{\sim}{k},\omega)\ P_b^*(\underset{\sim}{k}',\omega')\rangle\ , \tag{29}$$

$$\Psi_b(\underset{\sim}{k}|\underset{\sim}{k}',t|t') = \Phi_b(\underset{\sim}{k},\omega)\ \delta(\underset{\sim}{k}-\underset{\sim}{k}')\ \delta(\omega-\omega')\ , \tag{30}$$

respectively, where

$$P_b(\underset{\sim}{k},\omega) = (2\pi)^{-3/2} \int d\underset{\sim}{x} \int dt\ p(\underset{\sim}{x},t)\ \exp[i(\underset{\sim}{k}\cdot\underset{\sim}{x}-\omega t)]\ , \tag{31a}$$

$$\Psi_s(\underset{\sim}{k}|\underset{\sim}{k}',\omega|\omega') =$$

$$(2\pi)^{-3} \int d\underset{\sim}{x} \int dt \int d\underset{\sim}{x}' \int dt' \; \psi_b(\underset{\sim}{x}|\underset{\sim}{x}',t|t') \exp[i(\underset{\sim}{k}\cdot\underset{\sim}{x}-\underset{\sim}{k}'\cdot\underset{\sim}{x}'-\omega t+\omega' t')], \tag{31b}$$

$$\Phi_b(\underset{\sim}{k},\omega) = (2\pi)^{-3/2} \int d\underset{\sim}{x} \int dt \; \phi_b(\underset{\sim}{x},t) \exp[i(\underset{\sim}{k}\cdot\underset{\sim}{x}-\omega t)] \; . \tag{31c}$$

The quantity $\Phi_b(\underset{\sim}{k},\omega)$ is dubbed the spectral density of the pressure field. By definition, a pressure field that has a spectral density description is stationary, both spatially and temporally. If one assumes that the test external drive $P_e^{\nu}(\underset{\sim}{k},\omega)$ stated in Equation (24) is stationary, both spatially and temporally, then from this equation and Equation (30), one obtains

$$\langle|q|^2\rangle = \int d\underset{\sim}{k} \int d\omega \; W(\underset{\sim}{k},\omega) \; \Phi_e^{\nu}(\underset{\sim}{k},\omega) \; , \tag{32a}$$

$$\langle|q_{\ell}(h_{\ell})|^2\rangle = \int d\underset{\sim}{k} \int d\omega \; W(\underset{\sim}{k},\omega) \; W_{\ell}(\underset{\sim}{k},\omega) \; \Phi_e^{\nu}(\underset{\sim}{k},\omega) \; , \tag{32b}$$

$$\langle|q_{\ell}^{\nu}(h_{\ell})|^2\rangle = \int d\underset{\sim}{k} \int d\omega \; W(\underset{\sim}{k},\omega) \; W_{\ell}^{\nu}(\underset{\sim}{k},\omega) \; \Phi_e^{\nu}(\underset{\sim}{k},\omega) \; , \tag{32c}$$

respectively, where

$$\langle P_e^{\nu}(\underset{\sim}{k},\omega) \; P_e^{\nu *}(\underset{\sim}{k}',\omega')\rangle = \Phi_e^{\nu}(\underset{\sim}{k},\omega) \; \delta(\underset{\sim}{k}-\underset{\sim}{k}') \; \delta(\omega-\omega') \; , \tag{33}$$

$$W(\underset{\sim}{k},\omega) = |F(\underset{\sim}{k},\omega)|^2 \quad ; \quad W(\underset{\sim}{k},\omega) = W_a(\underset{\sim}{k},\omega) \; W_b(\underset{\sim}{k},\omega) \; ;$$

$$W_a(\underset{\sim}{k},\omega) = |F_a(\underset{\sim}{k},\omega)|^2 \quad ; \quad W_b(\underset{\sim}{k},\omega) = |F_b(\underset{\sim}{k},\omega)|^2 \; , \tag{34}$$

$$W_{\ell}(\underset{\sim}{k},\omega) = |F_{\ell}(\underset{\sim}{k},\omega)|^2 \quad , \tag{35a}$$

$$W_{\ell}^{\nu}(\underset{\sim}{k},\omega) = |F_{\ell}^{\nu}(\underset{\sim}{k},\omega)|^2$$

$$= U[1-k_{\nu}^2] + \exp[-2h_{\ell}^{\nu}(\kappa_{\nu}^2-1)^{1/2}]\ U[(k_{\nu}^2)] \ ; \quad k_{\nu}^2 = (kc_{\nu}/\omega) \tag{35b}$$

The quantities $W_a(\underset{\sim}{k},\omega)$, $W_b(\underset{\sim}{k},\omega)$, and $W_{\ell}(\underset{\sim}{k},\omega)$ may be dubbed the filtering actions of the array, the boundary, and the blanket, respectively [4]. In Equation (32), the outputs are given in terms of what is commonly referred to as the mean-square-values of the outputs.

Before turning to consider specific pressure fields of interest, it may be useful to state briefly a point of order. An array of transducers designed to decipher the wavevector distribution of a given field is dubbed a wavevector filter. Often an array designed to decipher the spectral distribution of a given field is dubbed a wavevector filter under the assumption that a frequency filter is readily acquired and, therefore, its inclusion needs no special mention. A pressure wavevector filter is, then, an array of pressure transducers, the filtering function, and/or the filtering action of which is shaped, in spectral space, with the specific intent of acquiring information relating to the pressure field described in spectral space. An array of transducers that is designed to acquire information relating to a field described in the spatial domain may thus be dubbed a spatial filter. In summary, the designation of an array of transducers, a wavevector, or a spatial filter indicates the operational purpose for which the array was designed.

V. PRESSURE FIELD OF A TURBULENT BOUNDARY LAYER AND OTHER STRAY PRESSURE FIELDS

The pressure field $p_t(\underset{\sim}{x},t)$ of a turbulent boundary layer is one of those pressure fields for which linear characterization is too complex to describe and one

commonly describes this pressure field in a quadratic and statistical form. It is also customary to assume that, at least over a spatial extent of interest, the pressure field of a turbulent boundary layer is stationary, both spatially and temporally, so that

$$\psi_t(\underset{\sim}{x}|\underset{\sim}{x}',t|t') = \langle p_t(\underset{\sim}{x},t)\ p_t^*(\underset{\sim}{x}',t')\rangle = (2\pi)^{-3/2}\ \phi_t(\underset{\sim}{x}-\underset{\sim}{x}',t-t')\ , \tag{36a}$$

$$\Psi_t(\underset{\sim}{k}|\underset{\sim}{k}',\omega|\omega') = \langle P_t(\underset{\sim}{k},\omega)\ P_t^*(\underset{\sim}{k}',\omega')\rangle = \Phi_t(\underset{\sim}{k},\omega)\ \delta(\underset{\sim}{k}-\underset{\sim}{k}')\ \delta(\omega-\omega')\ . \tag{36b}$$

Often on surfaces on which turbulent boundary layers form, stray pressure fields also exist. That is, on a boundary in addition to the turbulent boundary layer pressure field $p_t(\underset{\sim}{x},t)$, there may exist other pressure fields $\sum_s p_s(\underset{\sim}{x},t)$ so that the pressure field on the boundary $p_b(\underset{\sim}{x},t)$ is given by

$$p_b(\underset{\sim}{x},t) = p_t(\underset{\sim}{x},t) + \sum_s p_s(\underset{\sim}{x},t)\ . \tag{37}$$

Seldom are the various components of the pressure fields correlated. If one assumes these various components to be uncorrelated, one may derive from Equation (37) the quadratic and statistical forms

$$\psi_b(\underset{\sim}{x}|\underset{\sim}{x}',t|t') = \psi_t(\underset{\sim}{x}|\underset{\sim}{x}',t|t') = \sum_s \psi_s(\underset{\sim}{x}|\underset{\sim}{x}',t|t')\ . \tag{38}$$

If all the various components are assumed to be stationary, both spatially and temporally, then Equation (38) can be written in the form

$$\phi_b(\underset{\sim}{x}-\underset{\sim}{x}',t-t') = \phi_t(\underset{\sim}{x}-\underset{\sim}{x}',t-t') + \sum_s \phi_s(\underset{\sim}{x}-\underset{\sim}{x}',t-t')\ . \tag{39}$$

In spectral space, Equation (39) can be stated in the form

$$\Psi_b(\underset{\sim}{k}|\underset{\sim}{k}',\omega|\omega') = \Phi_b(\underset{\sim}{k},\omega)\ \delta(\underset{\sim}{k}-\underset{\sim}{k}')\ \delta(\omega-\omega') \quad ;$$

$$\Phi_b(\underset{\sim}{k},\omega) = \Phi_t(\underset{\sim}{k},\omega) + \sum_s \Phi_s(\underset{\sim}{k},\omega) \ . \tag{40}$$

The detailed nature of the spectral density $\Phi_t(\underset{\sim}{k},\omega)$ of the pressure field in a turbulent boundary layer is not known. Only some gross description of that spectral density is available. It is thus possible to describe the spectral density $\Phi_t(\underset{\sim}{k},\omega)$ in a simple representative manner [5]

$$\Phi_t(\underset{\sim}{k},\omega) = \Phi_o(\omega)\ \Phi_1(k_1,\omega)\ \Phi_2(k_2,\omega) \ ; \tag{41a}$$

$$\Phi_o(\omega) \equiv \Phi_o'(\omega\delta^*/U_c) \ ; \ \Phi_1(k_1,\omega) \equiv \Phi_1'(k_1U_c/\omega); \ \Phi_2(k_2,\omega) \equiv \Phi_2'(k_2U_c/\omega) \tag{41b}$$

$$\Phi_1(k_1,\omega) = \Phi_n(k_1,\omega) + \Phi_c(k_1,\omega) \ ; \tag{41c}$$

$$\Phi_n(k_1,\omega) = (a)[\alpha^2 + (1+|k_1U_c/\omega|)^2]^{-1} \tag{41d}$$

$$\Phi_c(k_1,\omega) = [\alpha^2+(1-k_1U_c/\omega)^2]^{-1} - [\alpha^2 + (1+|k_1U_c/\omega|)^2]^{-1} \tag{41e}$$

$$\Phi_2(k_2,\omega) = \beta^2[\beta^2 +(k_2U_c/\omega)^2]^{-1} \ . \tag{41f}$$

Assigning a strength factor Φ_o and a pair of factors Φ_1 and Φ_2, the spectral density $\Phi_t(\underset{\sim}{k},\omega)$ is factorized. The pair of factors Φ_1 and Φ_2 allows for the separation between the two principal directions; the flow is designated to be in the

x_1-direction and the convection speed of the turbulent boundary layer is designated U_c. The factor $\Phi_1(k_1,\omega)$ is assigned two terms, the convective part $\Phi_c(k_1,\omega)$ and the nonconvective part $\Phi_n(k_1,\omega)$. The nonconvective part is adjustable in that the parameter (a) is an unspecified constant; the nonconvective part of the spectral density can be made to vanish by setting (a) equal to zero. The parameters α and β are usually assumed to be such that $\alpha \approx 10^{-1}$ and $\beta \approx 3\alpha$; a more precise designation of α and β could imply that the description of the spectral density $\Phi_t(\underset{\sim}{k},\omega)$, as stated in Equation (41), is more thorough than is intended. A sketch that depicts the form of the spectral density $\Phi_t(\underset{\sim}{k},\omega)$, as stated analytically in Equation (41), is given in Figure 3.

If one knows the nature of a stray pressure field, its spectral density can be similarly stated. Thus, in wind or water tunnels one knows that in addition to the pressure field of a turbulent boundary layer, grazing acoustic pressure fields that propagate in the direction of flow are likely to be generated. A description that typifies such pressure fields may take the form [5]

$$\Phi_a(\underset{\sim}{k},\omega) = \Phi_{a+}(k_2,\omega)\ \delta[k_1-(\omega/c_\nu)] + \Phi_{a-}(k_2,\omega)\ \delta[k_1+(\omega/c_\nu)], \tag{42}$$

where c_ν is the speed of sound in the (ν)-fluid. A sketch that depicts the form of $\Phi_a(\underset{\sim}{k},\omega)$ as stated analytically in Equation (42) is given in Figure 4. Also, resonance vibration fields may be excited in the panels usually found in the walls of the test section of such wind or water tunnels. These vibrational fields would cause pressure fields to be generated on the boundary. The description that may typify such pressure fields may take the form [5]

$$\Phi_p(\underset{\sim}{k},\omega) = \Phi_{p+}(k_2,\omega)\ \delta[k_1-(\omega/c_p)] + \Phi_{p-}(k_2,\omega)\ \delta[k_1+(\omega/c_p)]. \tag{43}$$

where c_p is the free wave flexural speed in the panels. It is assumed in Equation (43) that the resonant vibration of the panel is predominantly confined to the direction of the flow. A sketch that depicts the form of $\Phi_p(\underset{\sim}{k},\omega)$ as stated analytically in Equation (43) is given in Figure 5. Similarly, one may visualize other stray pressure fields and typify their spectral density in the manner in which Equations (42) and (43) were constructed. However, since the experimental measurements to be discussed were performed in a water-tunnel-like environment, it is likely that the stray pressure fields could be substantially accounted for by the spectral density $\Phi_s(\underset{\sim}{k},\omega)$ so that

$$\Phi_s(\underset{\sim}{k},\omega) = \Phi_a(\underset{\sim}{k},\omega) + \Phi_p(\underset{\sim}{k},\omega) \ . \tag{44}$$

It is assumed then that the spectral density $\Phi_b(\underset{\sim}{k},\omega)$ of the pressure field on the boundary of the test section in the experimental setup is given by

$$\Phi_b(\underset{\sim}{k},\omega) \simeq \Phi_t(\underset{\sim}{k},\omega) + \Phi_s(\underset{\sim}{k},\omega) \quad ; \quad \Phi_s = \Phi_a + \Phi_p \ , \tag{45}$$

with the terms on the right defined more explicitly in Equations (41) through (43). A sketch that depicts the composite form of $\Phi_b(k,\omega)$ as stated analytically in Equation (45) is given in Figure 6. [Cf. Equations (41) through (43).] The array of pressure transducers that is flush mounted in the walls of the test section would then respond to the pressure field whose spectral density is $\Phi_b(\underset{\sim}{k},\omega)$. Using the formalism just developed, what is the output of the array? In particular, what is this output when the array is that deployed in the experiment of concern?

VI. FILTERING ACTION OF A TYPICAL WAVEVECTOR FILTER

Before determining the array output, one may inquire as to the nature of the filtering performed by the array. Since the driving field on the boundary is assumed to possess a spectral density, it is the filtering action of the array that one would desire to know [see Equation (32)]. It is also assumed that the transducers in the array are nominally identical [4]. Under this latter assumption, one may cast the filtering action of the array in the form [4,5]

$$W_a(\underset{\sim}{k},\omega) = W_s(\underset{\sim}{k},\omega)\, W_p(\underset{\sim}{k},\omega) \ , \tag{46}$$

where $W_p(\underset{\sim}{k},\omega)$ is the filtering action of an equivalent array, except that the transducers are assumed to be point transducers placed at the central positions of the actual transducers, and $W_s(\underset{\sim}{k},\omega)$ is the filtering action of a single transducer. For example, the transducers of the arrays deployed in the experiment of concern here were aligned in the x_1-direction (direction of flow), were equi-spaced, and their outputs were summed in phase (+ + mode) and alternatively out of phase (+ - mode). The arrays are typified in a sketch in Figure 7. For this array configuration one may show that [1]

$$W_p(\underset{\sim}{k},\omega) = W_{p_1}(k_1,\omega)\, W_{p_2}(k_2,\omega) \quad ; \quad W_{p_2}(k_2,\omega) \equiv 1 \ , \tag{47a}$$

$$W_{p_1}(\underset{\sim}{k},\omega) = \begin{cases} \sin^2\{N(k_1 d-\omega\tau)/2\}\ [N^2\sin^2\{(k_1 d-\omega\tau)/2\}]^{-1} \ , & (47b) \\ \sin^2\{N(k_1 d-\omega\tau)/2\}\ [N^2\cos^2\{(k_1 d-\omega\tau)/2\}]^{-1} \ , & (47c) \\ \cos^2\{N(k_1 d-\omega\tau)/2\}\ [N^2\cos^2\{(k_1 d-\omega\tau)/2\}]^{-1} \ , & (47d) \end{cases}$$

where d is the spacing and τ is the time delay parameter. Equation (47b) represents a situation in which adjacent transducers are similarly polarized (+ + mode), Equation (47c) represents a situation in which adjacent transducers are oppositely polarized (+ - mode) and the number N of transducers is even, Equation (47d) represents a situation in which adjacent transducers are oppositely polarized (+ - mode) and the number N of transducers is odd, and in each of the three cases the outputs of the transducers are simply summed to give the output of the array. Also, as an example, the single transducer is assumed to be rectangular in shape and of uniform point reacting sensitivity with one side lying in the x_1-direction as indicated in Figure 7. For this type of transducer one may show that [1]

$$W_s(\underset{\sim}{k},\omega) = W_o(\omega)\, W_{os}(\underset{\sim}{k}) \quad ; \quad W_{os}(\underset{\sim}{k}) = W_{s_1}(k_1)\, W_{s_2}(k_2) \quad ;$$

$$W_{s\alpha}(k_\alpha) = \sin^2(k_\alpha \gamma_\alpha d/2)\, [(k_\alpha \gamma_\alpha d/2)^2]^{-1} \quad , \quad \alpha = 1 \text{ or } 2 \, , \tag{48}$$

where $W_o(\omega)$ is the frequency filtering action of the transducer and any frequency filter that may be interjected in the output circuit; γ_1 and γ_2 are linear scale factors in the x_1- and x_2-directions, respectively, of the sides of the rectangular transducer as compared with the spacings between adjacent transducers. In the experiment of concern here, the frequency filtering action $W_o(\omega)$ is assumed to be that of a narrow band, e.g., (1/10) octave band, centered about the center frequency ω_o. The skirts of the filter are considered low as indicated in Figure 8. Also in the experiment of concern here, the number of transducers in a typical array was 12; N = 12. A typical form of $W_p(\underset{\sim}{k},\omega)$ for the array is depicted in Figure 9. In Figure 10 is depicted a typical form of $W_{os}(\underset{\sim}{k})$ for a rectangular transducer. The filtering action factor $W_{o\alpha}(\underset{\sim}{k},\omega)$ is defined so that

$$W_a(\underset{\sim}{k},\omega) = W_o(\omega)\, W_{oa}(\underset{\sim}{k},\omega) \quad ; \quad W_{oa}(\underset{\sim}{k},\omega) = W_{os}(\underset{\sim}{k},\omega)\, W_p(\underset{\sim}{k},\omega) \ . \tag{49}$$

From Figures 9 and 10 and Equation (49), the nature of the filtering action factor $W_{oa}(\underset{\sim}{k},\omega)$ is depicted in Figure 11. It is important to note that if the nominal properties of the transducers and the spacings between them as stated above are not strictly adhered to, the result is that the discrimination of the filtering action is not as good as that depicted in Figure 11. The loss of discrimination is manifested by peaks and valleys, being neither as high and deep, respectively, nor as sharp. The loss in definition in the filtering action just discussed is most pronounced in those spectral ranges defined by coordinates that are of the same and higher linear sizes than the variations and deviations from nominality. Thus, if the spacing in the x_1-direction admits to variations of the order of Δx_1, the spectral range in which even major peaks lose substantial definition covers the range $(k_1 \Delta x_1) > 1$ in the k_1-coordinate of spectral space. Yet it is noted that the integrated acceptance A of the array, namely

$$A(d,\gamma_1,\gamma_2,\tau,\omega_o) = \int d\underset{\sim}{k} \int d\omega\, W_a(\underset{\sim}{k},\omega) \ , \tag{50}$$

remains substantially invariant to these variations and deviations [4].

Now that the natures of the spectral density of a typical pressure field and the filtering action of a typical array are grossly known and expressed, the gross values of the output of the array may be ascertained [Equation (32a)]. Then aspects of the pressure fields and the performance of the array as a spectral filter can be investigated. Further, if blankets are placed on the boundary, the influence of these blankets on the outputs of the array may then be ascertained [Equation (32b) or (32c)] by inserting the appropriate expression for the filtering actions of the blankets [e.g., Equation (35b)]. The investigation of the nature of this influence

has a significant purpose for this experiment. Therefore, the analysis developed in this paper is cast in a form that would assist with the interpretation of the data obtained.

VII. TYPICAL EXPERIMENTAL PROCEDURES AND DATA ACQUISITION

To retain simplicity it is assumed that the boundary is of uniform impedance and that the pressure field on it possesses a spectral density. Under these assumptions, Equation (32) is valid for the determination of the output of an array that is flush mounted in the boundary in the manner prescribed therein. Using the description of the spectral density of the pressure field on the boundary given in Section V and the filtering action of the spectral filter that is flush mounted in that boundary given in Section VI, the output $\langle|q|^2\rangle$ of that filter can be stated in the form

$$\langle|q|^2\rangle = \langle|q_a|^2\rangle + \langle|q_p|^2 + \langle|q_t|^2\rangle \ , \tag{51}$$

$$\langle|q_\alpha|^2\rangle \simeq A_\alpha(\omega_o)\ W_{s1}(\omega_o/c_\alpha)\ W_{p1}(\omega_o/c_\alpha) \quad ; \quad \alpha = a \text{ or } p \text{ and } c_a = c_\nu \ , \tag{52}$$

$$A_\alpha(\omega_o) = \int dk_2 \int d\omega\ W_o(\omega)\ W_{s_2}(k_2)\ [\Phi_{\alpha+}(k_2,\omega) + \Phi_{\alpha-}(k_2,\omega)], \tag{53}$$

$$\langle|q_t|^2\rangle = A_t(\omega_o)\ [B_t(\omega_o) + C_t(\omega)] \ , \tag{54}$$

$$A_t(\omega) = \int d\omega\ W_o(\omega)\ \Phi_o'(\omega\delta^*/U_c) \ , \tag{55a}$$

$$B_t(\omega_o) = \int d\underset{\sim}{k}\ W_{oa}(\underset{\sim}{k},\omega_o)\ \Phi_1(k_1,\omega_o)\ \Phi_2(k_2,\omega) \quad ; \quad k<(\omega_o/c_\nu) \ , \tag{55b}$$

$$C_t(\omega_o) = \int d\underset{\sim}{k}\ W_{oa}(\underset{\sim}{k},\omega_o)\ \Phi_1(k_2,\omega_o)\ \Phi_2(k_2,\omega) \quad ; \quad k>(\omega_o/c_\nu) \ , \tag{55c}$$

where $k^2 = k_1^2 + k_2^2$. It is assumed in stating these equations that the frequency filtering action represents a narrow enough frequency band and the skirts of the filter are low enough. The filtering action of the blankets considered in this section is assumed to be ideal so that the form of their filtering action is prescribed in Equation (35b). It is also assumed that the pressure fields on the boundary induced by the vibrational fields on the boundary are not changed by the presence of a blanket. In addition, it is assumed that the spectral distributions Φ_1 and Φ_2 of the pressure field in a turbulent boundary layer are not significantly different whether they form on a boundary or on a blanket that may be placed on the boundary. However, provision is made to allow the frequency spectral density function to change from $\Phi_o'(\omega\delta^*/U_c)$ to $\Phi_{o\ell}'(\omega\delta^*/U_c)$ if a blanket is introduced. Under these assumptions, the output of the spectral filter in the presence of a blanket may be stated

$$\langle |q_\ell|^2 \rangle = \langle |q_{a\ell}|^2 \rangle + \langle |q_{p\ell}|^2 \rangle + \langle |q_{t\ell}|^2 \rangle \ , \tag{56}$$

$$\langle |q_{\alpha\ell}|^2 \rangle = \langle |q_\alpha|^2 \rangle \quad ; \quad \alpha = a \text{ or } p \ , \tag{57}$$

$$\langle |q_{t\ell}|^2 \rangle = A_{t\ell}(\omega_o)\ [B_{t\ell}(\omega_o) + C_{t\ell}(\omega_o)] \ , \tag{58}$$

$$A_{t\ell}(\omega_o) = \int d\omega\ W_o(\omega)\ \Phi_{o\ell}(\omega\delta^*/U_c) \ , \tag{59a}$$

$$B_{t\ell}(\omega_o) = B_t(\omega_o) \ , \tag{59b}$$

$$C_{t\ell}(\omega_o) = \int d\underset{\sim}{k}\ W_{oa}(\underset{\sim}{k},\omega_o)\ W_\ell^\nu(\underset{\sim}{k},\omega_o)\ \Phi_1(k_1,\omega_o)\ \Phi_2(k_2,\omega_p) \ ; \ k>(\omega_o/c_\nu) \tag{59c}$$

[Cf. Equations (51) through (55).] It is noted that were a turbulent boundary layer a truly external drive so that

$$\Phi_{o\ell}(\omega\delta^*/U_c) = \underset{(60)}{\Phi_o}(\omega\delta^*/U_c), \text{ then } A_{t\ell}(\omega_o) = A_t(\omega_o). \tag{60}$$

From equations (51) and (56), one may define a blanket modification factor L so that

$$L = \langle|q_\ell|^2\rangle/\langle|q|^2\rangle \ , \tag{61}$$

in which the filtering conditions and mode of operation of the filter remain fixed. The only change is the introduction of a blanket. Of course the factor L is a function of these conditions and also of the blanket thickness h_ℓ. From Equations (51) through (61), one obtains

$$L = [R_\ell + E_{t\ell}]\,[R+1]^{-1} \ ; \ E_{t\ell} = \bar{A}_{t\ell}\,\bar{C}_{t\ell} \ ; \ \bar{A}_{t\ell} = A_{t\ell}/A_t \ ;$$

$$\bar{C}_{t\ell} = C_{t\ell}/C_t \ ; \ \bar{B}_t = B_t/C_t \ ; \ B_t = B_{t\ell} \ , \tag{62}$$

where

$$R_\ell(\omega_o) = R_a(\omega_o) + R_p(\omega_o) + \bar{A}_{t\ell}(\omega_o)\,\bar{B}_t(\omega_o) \ , \tag{63a}$$

$$R(\omega_o) = R_a(\omega_o) + R_p(\omega_o) + \bar{B}_t(\omega_o) \ , \tag{63b}$$

$$R_\alpha(\omega_o) = \bar{A}_\alpha(\omega_o)\,W_{s1}(\omega_o/c_\alpha)\,W_{p1}(\omega_o/c_\alpha) \ ;$$

$$\bar{A}_\alpha = (A_\alpha/A_tC_t) \ . \tag{64}$$

The blanket modification factor L is the quantity destined to be measured in an experiment. However, it is the determination of the quantity $E_{t\ell}$ that is of special interest. This latter quantity is related directly to the effectiveness of the blanket in inhibiting spectral components in the pressure field of a turbulent boundary layer from reaching the covered boundary. The quantity $E_{t\ell}$ may thus be dubbed the blanket effectiveness factor. The blanket is beneficially effective if $E_{t\ell}$ is less than unity; $E_{t\ell} < 1$, and is more effective the smaller the value of $E_{t\ell}$. It is clear from Equation (62) that the blanket effectiveness factor is composed of two factors; the first factor $\bar{A}_{t\ell}$ may be dubbed the frequency factor and the second $\bar{C}_{t\ell}$ may be dubbed the wavevector factor [Cf. Equations (59a) and (59c)]. A blanket may then be beneficially effective either because $\bar{A}_{t\ell}$ is less than unity, $\bar{C}_{t\ell}$ is less than unity, or both are less than unity. Invariably $\bar{C}_{t\ell}$ is less than unity. Such a definitive statement cannot be made with respect to the frequency factor $\bar{A}_{t\ell}$.[1] If, however, the turbulent boundary layer is truly an external drive as stated in Equation (60), then $\bar{A}_{t\ell} = 1$.

The prime purpose for the experiment of concern here was to determine the blanket effectiveness factor, and a closer examination and interpretation of this factor is thus warranted. Of particular interest is the experimental procedure. A wavevector filter is placed in a boundary of the test section of a water tunnel. A major acceptance region in the filtering action of the filter is placed at $k_1 = (\pi/d)$ when the filter is operated in the (+ −) mode and at $k_1 = (2\pi/d)$ when operated in the (+ +) mode; intermediate time delays are not used. A turbulent boundary layer is formed on the boundary as a result of the flow that is imposed on the fluid. The flow reaches a steady speed U. This speed is assumed to be highly subsonic; $(U/c_\nu) << 1$. The frequency filter in the circuit of the output of the transducer is manipulated so that at the center frequency ω_o the peak in the

spectral density of the pressure field is coincidental with the major acceptance regions just defined. The locations are ascertained by gross estimates and then by finely tuning the center frequency ω_o so that a maximum is attained in the output of the array. It is conjectured that at this setting of the spectral filter, and in the absence of a blanket, the output $\langle|q_t|^2\rangle$ generated by the turbulent boundary layer of concern here would substantially exceed the output $\langle|q_s|^2\rangle$ generated by the stray pressure fields. More precisely, it is assumed that $R \ll 1$ in Equation (62). This is achievable if the turbulent boundary layer is subsonic, $U_c \ll c_\nu$, and and noise control procedures were applied to minimize the strengths of the stray pressure fields. It is noted in this connection that inherently $\bar{B}_t(\omega_o) \ll 1$ in a highly subsonic turbulent boundary layer. It is also noted that if $(NU_c/c_\alpha) \ll \pi$, the contribution to R by the (α)th stray pressure field in the (+ −) mode is substantially less than that in the (+ +) mode of operation of the wavevector filter. This is so because in the (+ +) mode a major acceptance region in the filtering action of the filter lies at the origin $|k| \simeq 0$, while in the (+ −) mode, at worst, a minor acceptance region lies at the origin. It is then assumed here that even $[R(\omega_o)]_{(+\ +)} \ll 1$, and this condition ensures that $[R(\omega_o)]_{(+\ -)} \ll 1$.[2] Under the assumption that the contribution by the turbulent boundary layer is dominant in the output of the array and that the flow is highly subsonic so that $R(\omega_o) \ll 1$, the locations of the spectral region at which the maxima may be defined are

Coordinate	(+ −) mode	(+ +) mode
$k_1 \rightarrow k_{10}$	(π/d)	$(2\pi/d)$
$k_2 \rightarrow k_{20}$	0	0
$\omega \rightarrow \omega_o$	$(\pi U_c/d)$	$(2\pi U_c'/d)$

(65)

The convection speeds are dependent on the wavenumber k_1 and, therefore, a distinction has to be made with respect to the convection speed U_c when the (+ −) mode is operative, $U_c = U_c(\pi/d,0)$, and U_c' when the (+ +) mode is operative, $U_c' = U_c'(2\pi/d,0)$. Thus, U_c may, in general, be different from U_c'. When the blanket is placed on the boundary so that the turbulent boundary layer is displaced away from the boundary in which the array is flush mounted, the setting of the spectral filter specified in Equation (65) remains, by definition, intact. The blanket modification factor L is ascertained as a function of the thickness of the blanket at the same setting that is established by the procedure that led to Equation (65). Then the center frequency ω_o is fixed either at $(\pi U_c/d)$ or $(2\pi U_c'/d)$; the center wavenumber k_{10} is either at (π/d) or $(2\pi/d)$, and the center wavenumber k_{20} is at 0, respectively. It is then possible and convenient to designate parameters and quantities that pertain to the (+ −) mode of the array by superscript (−) and those that pertain to the (+ +) mode of the array by superscript (+); e.g., $\omega_o^- = (\pi U_c/d)$, $\omega_o^+ = (2\pi U_c'/d)$, $k_{10}^- = (\pi/d)$, $k_{10}^+ = (2\pi/d)$, $k_{20}^- = 0$, $k_{20}^+ = 0$, $A(\omega_o^-) = A^-(\omega_o^-)$, etc. In particular, and from Equation (62), one obtains

$$L(k_{10}h_\ell,\omega_o) = [R_\ell(\omega_o) + E_{t\ell}(k_{10}h_\ell,\omega_o)]\ [R(\omega_o)+1]^{-1}\ , \tag{66a}$$

$$L^-(k_{10}^-h_\ell,\omega_o^-) = [R_\ell^-(\omega_o^-) + E_{t\ell}^-(k_{10}^-h_\ell,\omega_o^-)]\ [R^-(\omega_o^-)+1]^{-1}\ , \tag{66b}$$

$$L^+(k_{10}^+h_\ell,\omega_o^+) = [R_\ell^+(\omega_o^+) + E_{t\ell}^+(k_{10}^+h_\ell,\omega_o^+)]\ [R^+(\omega_o^+)+1]^{-1}\ , \tag{66c}$$

It is noted that the blanket modification factor L and the blanket effectiveness factor $E_{t\ell}$ are now specified with respect to a specific spectral region; here that region is defined by $\{k_{10},0,\omega_o\}$. [In the (+ −) mode the spectral region

is defined by $\{k_{10}^{-},0,\omega_o^{-}\}$ and in the (+ +) mode by $\{k_{10}^{+},0,\omega_o^{+}\}$.] It is recalled that in this paper it is assumed that $R(\omega_o) << 1$ so that Equation (66) can be approximated to read

$$L(k_{10}h_\ell,\omega_o) \simeq R_\ell(\omega_o) + E_{t\ell}(k_{10}h_\ell,\omega_o) \quad ; \quad R(\omega_o) << 1 \ . \tag{67}$$

$$\bar{C}_{t\ell}(k_{10}h_\ell,\omega_o) = S^{\nu}(h_\ell^{\nu o})/S^{\nu}(0) \quad , \tag{68a}$$

$$\bar{B}_t(\omega_o) + \bar{C}_{t\ell}(k_{10}h_\ell,\omega_o) = S(h_\ell^{\nu o})/S(0) \quad , \tag{68b}$$

where

$$S^{\nu}(h_\ell^{\nu o}) =$$

$$\int d\underset{\sim}{k} \exp\{-2h_\ell^{\nu o}(\kappa_{\nu o}^2-1)^{1/2}\} W_{o\alpha}(\underset{\sim}{k},\omega_o) U[k-(\omega/c_\nu)] \Phi_1(k_1,\omega_o) \Phi_2(k_2,\omega_o), \tag{69a}$$

$$S(h_\ell^{\nu o}) = \int d\underset{\sim}{k} \exp\{-2h_\ell^{\nu o}(\kappa_{\nu o}^2-1)^{1/2}\} W_{oa}(\underset{\sim}{k},\omega_o) \Phi_1(k_1,\omega_o) \Phi_2(k_2,\omega_o) \ , \tag{69b}$$

$$h_\ell^{\nu o} = (h_\ell \omega_o/c_\nu) \quad ; \quad \kappa_{\nu o} = (kc_\nu/\omega_o) \quad , \tag{69c}$$

$$R_\ell(\omega_o) = R_a(\omega_o) + R_p(\omega_o) + \bar{A}_{t\ell}(\omega_o) \bar{B}_t(\omega_o) \ , \tag{70a}$$

$$\bar{B}_t(\omega_o) = B_t(\omega_o)/A_t(\omega_o) << 1 \qquad \text{if } U << c_\nu \ , \tag{70b}$$

$$R_a(\omega_o) = \bar{A}_a(\omega_o) W_{s1}(\omega_o/c_\nu) W_{p1}(\omega_o/c_\nu) \quad ; \quad \bar{A}_a(\omega_o) << 1 \ , \tag{70c}$$

$$R_p(\omega_o) = \bar{A}_p(\omega_o) W_{s1}(\omega_o/c_p) W_{p1}(\omega_o/c_p) \quad ; \quad \bar{A}_p(\omega_o) << 1 \ . \tag{70d}$$

The inequalities in Equations (70c) and (70d) imply that adequate and successful noise control procedures were applied to the water tunnel in which the experiment was performed. From Equations (67) through (70), one obtains

$$L(k_{10}h_\ell,\omega_o) = R_a(\omega_o) + R_p(\omega_o) + \bar{A}_{t\ell}(\omega_o)\,\bar{B}_t(\omega_o) + \bar{A}_{t\ell}(\omega_o)\,\bar{C}_{t\ell}(k_{10}h_\ell,\omega_o)\ . \tag{71}$$

Equation (71) is the basic equation for designing a proper experiment, acquiring meaningful data, and interpreting that data. Significant progress can be achieved with this equation if the wavevector factor $\bar{C}_{t\ell}$ is estimated so that at least one of the two factors in the blanket effectiveness factor is available. That this factor can be computed in some detail is evident from Equation (68). At this stage, however, it may be useful to try to evaluate this factor even approximately. This would not only prepare the groundwork for such computations, but would also lead to understanding the significance of such evaluations without the clutter that usually accompanies extensive computations. In that spirit, a mean value estimate [6] is applied to Equation (69a). The application yields

$$\bar{C}_{t\ell}(k_{10}h_\ell,\omega_o) \simeq \exp(-2bk_{10}h_\ell) \quad ; \quad \bar{A}_{t\ell} = (A_{t\ell}/A_t)\ . \tag{72}$$

One may argue that, grossly, b is a constant of the order of unity, $b \simeq 1$. [Computations using Equation (68) and the spectral density stated in Equation (41) seem to support this argument.] Then from Equations (66) and (68), one obtains

$$L(k_{10}h_\ell,\omega_o) \simeq R_a(\omega_o) + R_p(\omega_o) + \bar{A}_{t\ell}(\omega_o)\,\bar{B}_t(\omega_o) + \bar{A}_{t\ell}(\omega_o)\exp(-2k_{10}h_\ell). \tag{73}$$

The meanings and interpretations of Equation (73) are depicted graphically in Figures 12 and 13.

It is observed that analytical estimates can be made of the employment of spectral filters to investigate the effectiveness of a blanket to inhibit spectral components in a turbulent boundary layer from reaching the boundary that the blanket covers. Such analytical estimates can be used in turn to design proper experimental setups and procedures, to decide the manner and extent of data acquisition, and to assist with the interpretation of the data. The analytical estimates represented in Equation (73), however, do more than that. The various limitations, conditions, and assumptions that were laid down in order to reach the equation may be used to advantage not only to explain idiosyncracies and controversies in the data, but also the measures that may be taken to resolve them. Thus, one may, within the formalism developed here, attempt to resolve such questions as: how important are deviations from stationarity; how essential are the impositions that the boundary is of uniform impedance; and what are the implications if the blanket is not ideal [7]? The answers to such questions lie outside the scope of this paper, but not outside the scope of the formalism that is developed herein.

It would be useful now to try to match data with the formalism. However, before making an attempt to cast the limited available data in the format prescribed by the analysis performed in this paper, it is in order to peruse and estimate the wavevector factor $\bar{C}_{t\ell}$ in the more elaborate, if not the more realistic, form specified in Equation (68).

VIII. TYPICAL EVALUATION OF THE WAVEVECTOR FACTOR $\bar{C}_{t\ell}$ AS A FUNCTION OF THE NORMALIZED THICKNESS OF THE BLANKET

A mean value estimate was applied to Equation (69a) to obtain the estimates for the blanket modification factor L stated in Equation (73) [6]. The graphical

interpretations of Equation (73) are depicted in Figures 12 and 13. To validate the range and nature of these estimates it is useful to perform the double integration and obtain the wavevector effectiveness factor $\bar{C}_{t\ell}$ directly of Equations (68) and (69). In spite of the simplification in the integrand obtained by the rough and gross approximations to the explicit nature of the functions involved thereof, numerical integration is nonetheless mandatory. To render the computational procedure easier, the factor $[\bar{B}_t + \bar{C}_{t\ell}]$ is evaluated rather than the factor $\bar{C}_{t\ell}$. Equations (47) through (49) are used for the filtering action factors of the array, and Equations (41a) through (41f) are used for the spectral density of the turbulent boundary layer. The results of the calculations are presented in Figure 14 for several values of the constant (a) in Equation (41d). The curves in Figure 14 correspond to those in Figures 12 and 13 [evaluated from Equation (73)] with $R_a = R_p = 0$. The essential characteristics of $\bar{C}_{t\ell}$ [or $\bar{B}_t + \bar{C}_{t\ell}$] in Figure 14 are seen to be commensurate with those of Figures 12 and 13. In particular, the wavevector effectiveness factor $\bar{C}_{t\ell}$ exhibits exponential variations in $k_{10}h_\ell$ until a limit is reached where substantially no further dependence on $k_{10}h_\ell$ occurs in $[\bar{B}_t + \bar{C}_{t\ell}]$; $[\bar{B}_t + \bar{C}_{t\ell}]$ saturates at a certain level as $k_{10}h_\ell$ increases beyond a certain value. It is apparent in Figure 14 that the saturation level and the value of $k_{10}h_\ell$ at which saturation commences, are different for the (+ +) mode and the (+ -) mode of operation of the array. This feature was observed and discussed earlier with respect to Figures 12 and 13. A difference of note between the corresponding curves in Figures 12 and 13 and Figure 14 relates to the more abrupt transition to saturation in the former than than in the latter; Equation (73) tends to exaggerate the transition to saturation of the factor $[\bar{B}_t + \bar{C}_{t\ell}]$. It is, therefore, concluded that, by and large the approximation in the derivation of Equation (73) and the salient features exhibited in Figures 12 and 13 are analytically viable representations.

IX. DESCRIPTION OF THE EXPERIMENT AND DATA

The experiments were performed in a quiet, blowdown, water facility at DTNSRDC. A schematic of the facility is shown in Figure 15. Water flows from the head tank through a 12-inch inside diameter pipe, a gate valve, a settling tank, a ball valve, and a 3-inch inside diameter test pipe. The flow exits underwater in a large receiving tank. All parts of the system from the head tank to the ball valve are heavy gauge steel and are mounted rigidly to steel or concrete bases. The test pipe is constructed of transparant Butyrate plastic with a 0.216-inch wall thickness. The test pipe is rigidly fixed and mechanically damped with sandbags along its length. The test section is 100 pipe diameters from the ball valve, ensuring fully developed turbulent flow. All joints are carefully aligned and the gate and ball valves were reworked to ensure smooth flow through them. Indeed, the ball valve required extensive modification and reworking to ensure a good internal alignment. Improper alignment usually results in the occurrence of cavitation at the higher water speeds. Such conditions did not occur during the experiment. The head tank can be supercharged with compressed air or evacuated. This results in a large range of mean flow speeds, up to about 60 ft/sec. Water speed can be measured by inference from pressure drop data or directly using an electromagnetic flowmeter. Water speed can be held constant to less than 1 percent of the desired speed, except when running only under gravity forces. Typical operation after filling the system is to supercharge the head tank to the desired pressure, open the pneumatically operated gate valve, wait a few moments for any resulting noise or vibration to settle down, then open the pneumatically operated ball valve. Water speed remains constant for about 1 to 5 minutes, depending on the speed. There are no external noise sources, such as pumps, operating during a run, and the continuously fed compressed air passes through a large muffler system prior

to entering the head tank. Background noise is usually the electronic noise of the miniature pressure transducers commonly employed in the measurements.

Figure 16 illustrates the test section employed in the present experiment. In order to ensure that the inside diameter remained constant for differing blanket thicknesses, individual brass test sections were constructed for each thickness. The test sections were 24-inches long with natural rubber of the desired thickness vulcanized to the interior. For the results reported here, two blanket thicknesses were used, 0.25 inches and 0.50 inches. A mounting slot was cut into the test sections to allow two specially constructed linear wavevector filter arrays to be mounted with their sensitive surfaces touching the inner side of the blankets in the plane of the inner boundary. Both wavevector filters were linear and constructed with 12 pressure sensing elements with a transverse dimension of $\gamma_2 d = 0.250$ inches. One had elements the widths of which were $\gamma_1 d = 0.150$ inches, while the other had elements the widths of which were $\gamma_1 d = 0.060$ inches in the flow direction. In each case, the center-to-center separation distance d was set so that $\gamma_1 = 2/3$. This setting eliminates the response peak at $k_{10} = 3\pi/d$ in the (+ -) mode.

Data were obtained at a number of mean flow speeds from 15 to 60 ft/sec with each of the two test sections and each of the two wavevector filter arrays. The data were amplified and recorded on magnetic tape. The signals were analyzed by passing all 12 channels of data into a specially constructed sum and difference instrument. The signals could then be simultaneously summed together in phase, (+ +) mode, or alternatively out of phase, (+ -) mode. This provided primary wavenumber response bands at $k_{10}^{+} = 0$ and at $k_{10}^{+} = 2\pi/d$ for the (+ +) mode and at $k_{10}^{-} = \pi d$ for the (+ -) mode. At each speed with no blanket in place, the data showed a clear peak where the response bands centered at k_{10}^{+} $2\pi/d$ and k_{10}^{-} π/d

were coincident with the convective part of the pressure field [where $\omega_o = k_{10}U_c$]. With the blankets in place, the peaks at these frequencies were dramatically reduced. The average reduction in the peaks at each speed was taken as the measure of the wavevector modification factor L as a function of the normalized blanket thickness $k_{10}h_\ell$. The preliminary results of the experiment with the above two blanket thicknesses are plotted in Figure 17. The trends of Figures 12 and 13 are evident in the data. The modification factor L is seen to decrease exponentially as $k_{10}h_\ell$ increases and then saturates as $k_{10}h_\ell$ increases beyond a certain value. This is seen to occur for both modes of operation. However, it is seen that L saturates sooner in the (+ +) mode than in the (+ −) mode. This is in agreement with the analytical development discussed in this paper. Values of R_a and R_p were not obtained, however, so that it is not possible to say with certainty whether the saturation is due to such extraneous sources or naturally due to the low wavenumber part of the pressure field in a turbulent boundary layer. An interesting aspect of the data occurs near $k_{10}h_\ell \to 0$. A line through the data does not extrapolate to zero. Rather, it extrapolates to an intercept off zero commensurate with Figures 12c, 12d, 13c, and 13d. The intercepts in Figures 12c, 12d, 13c, and 13d were explained on the basis that the strength $\Phi_o'(\omega_o\delta^*/U_c)$ of the spectral density in a turbulent boundary layer may change if the turbulent boundary layer is formed on a boundary of a blanketed surface as compared with that on a boundary of a bare surface. The data presented herein is consistent with such interpretation and indicates that an increase of about 10 dB may take place in $\Phi_o'(\omega_o\delta^*/U_c)$ with the prescribed change in the boundary. It is noted that such an increase diminishes the effectiveness of the blanket by a corresponding amount. Whether the data presented in Figure 17 is persistent and generally reproducible remains to be examined; further analysis of the records taken in this experiment is pending. It would also

be advantageous to acquire data in other experimental situations. Such examination would be helpful in attempting to further explore the true effectiveness of a blanket. It is hoped that the analytical tool developed in this paper may assist with the further analysis of the data already acquired and with the design of experiments in which fresh data could be meaningfully acquired.

X. REMARKS

1. Rumor has it, and fragmented theoretical and experimental evidence support it, that the nature of turbulent boundary layers may be dependent on the nature of the surfaces on which they form, even if the surfaces are hydraulically smooth; e.g., the nature of a turbulent boundary layer that forms on a rigid surface may be different from that which forms on a surface that is not rigid. In particular, the nature of a turbulent boundary layer that forms on a bare surface may be different from that which forms on the top surface of a blanket that covers the bare surface. The nature of a turbulent boundary layer is defined herein in terms of the function $\Phi_t(\underset{\sim}{k},\omega)$ which is assumed to be composed of three factors, as stated in Equation (41). Differences in the nature of turbulent boundary layers may involve either any one, any pair, or all three factors; no a priori specification for the differences is presently available.

The chief concern in this paper is the determination of the blanket effectiveness factor $E_{t\ell}$. Subsequently, it is shown that the experimental procedure is such that the factor is ascertained largely at the localized and specific spectral range; that range is defined by a major acceptance region in the filtering action of a spectral filter. It is assumed in this paper that the blanket effectiveness factor $E_{t\ell}$ is factorable into two parts $\bar{A}_{t\ell}$ and $\bar{C}_{t\ell}$; $E_{t\ell} = \bar{A}_{t\ell}\,\bar{C}_{t\ell}$. The first factor is assumed to be associated with the strength and frequency distribution of the spectral density of the pressure field in a turbulent boundary layer, and the

second factor is assumed to be associated with the wavevector distribution of this spectral density. A blanket is commonly assumed to be a wavevector filter in that it inhibits spectral components from reaching the boundary it covers according to the component's wavevector designation rather than its frequency designation. In that sense it is specified that $\bar{C}_{t\ell}$ is less than unity. However, implicit in this statement is the assumption that the wavevector distribution in the turbulent boundary layer remains substantially intact when it forms on the surface of the blanket rather than on the boundary that the blanket covers. Indeed, it is assumed that if a change occurs it is due to a change in the strength of the pressure field and not even in the frequency distribution in the turbulent boundary layer. In that sense it is specified that $\bar{A}_{t\ell}$ may change and that the change may occur either way, or not at all; either $\bar{A}_{t\ell} > 1$, $\bar{A}_{t\ell} < 1$ or $\bar{A}_{t\ell} = 1$. It is recognized that efforts and attempts are being made to cause changes in the nature of a turbulent boundary layer by introducing specific surfaces over which the turbulent boundary layers are to form. [Some aspects of such introductions were discussed in a recent Drag Reduction Symposium, September 13-17, 1982, held at the National Academy of Sciences, Washington, D.C.] Programs that support the efforts are directly related to the subject of this paper on the basis of both the analytical and experimental endeavors. Thus, for example, a blanket designer would benefit greatly if he knew how to manufacture a blanket that would not only be effective in decreasing $\bar{C}_t$ but also in decreasing substantially the value of $\bar{A}_{t\ell}$.

2. Subsequently it is argued that for the (+ +) mode $\omega_o \to \omega_o^+ \simeq (2\pi U_c'/d)$ and $W_p \to W_p^+ (2\pi U_c'/c_\alpha d)$, for the (+ −) mode $\omega_o \to \omega_o^- \simeq (\pi U_c/d)$ and $W_p \to W_p^- (\pi U_c/c_\alpha d)$, and $U_c' \simeq U_c$. Thus if one imposes that the flow is highly subsonic with respect to the speed c_α so that $(NU_c/c_\alpha) \ll \pi$, then it follows from Equation (47) that

$$[W_p^- / W_p^+] \simeq \begin{cases} (\pi U_c/c_\alpha)^2 \ll 1 \text{ if N is even} \\ (N)^{-2} \ll 1 \text{ if N is odd} \quad . \end{cases}$$

Thus, if (U_c/c_α) is of the order of 10^{-2} and assuming that $A_\alpha^+(\omega_o^+) \simeq A_\alpha^-(\omega^-{}_o)$ one may conclude that

$$[R_\alpha^-(\omega_o^-)/R_\alpha^+(\omega_o^+)] \simeq \begin{cases} 10^{-3} \text{ if N is even} \\ (N)^{-2} \text{ if N is odd} \; . \end{cases}$$

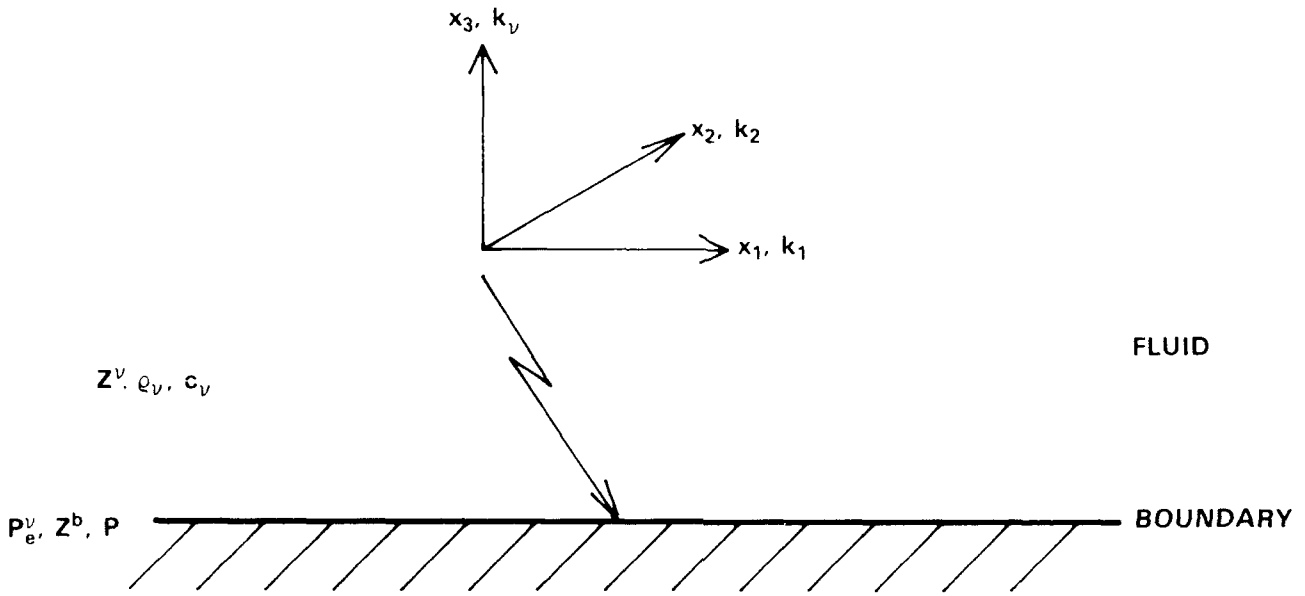

Figure 1 - Coordinate System

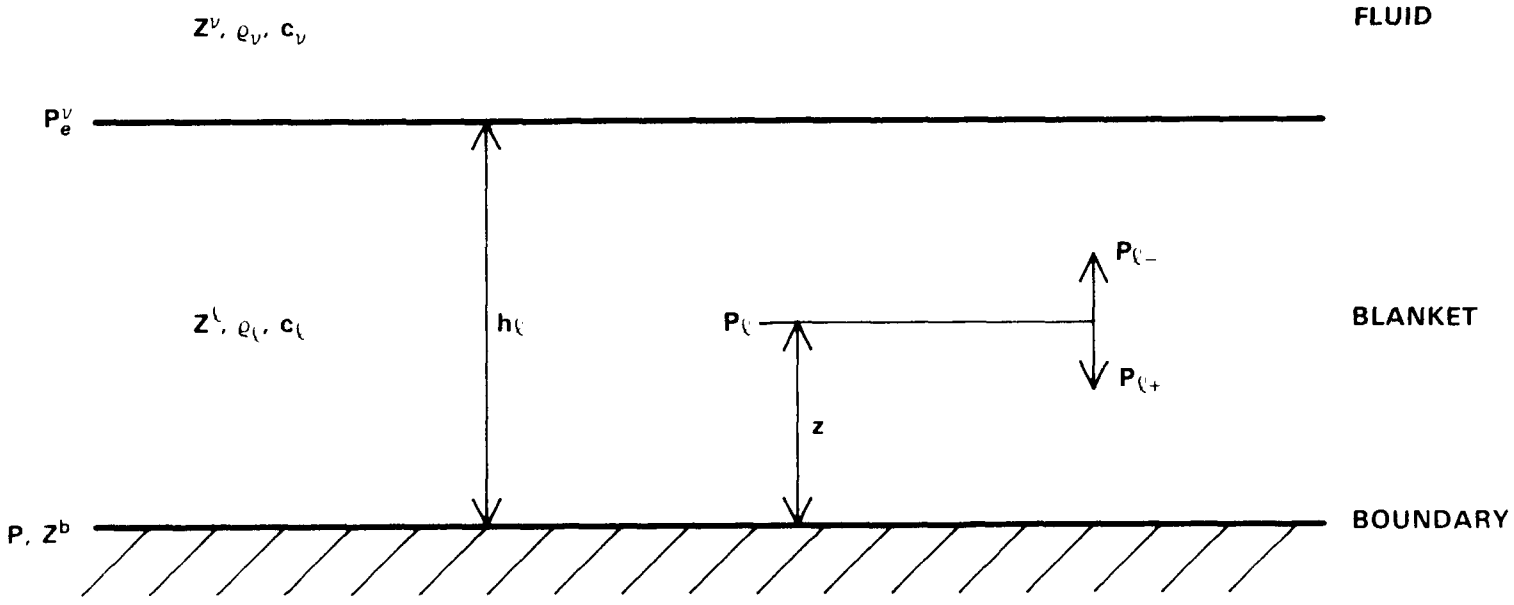

Figure 2 - Fluid-Blanket-Boundary Relationships

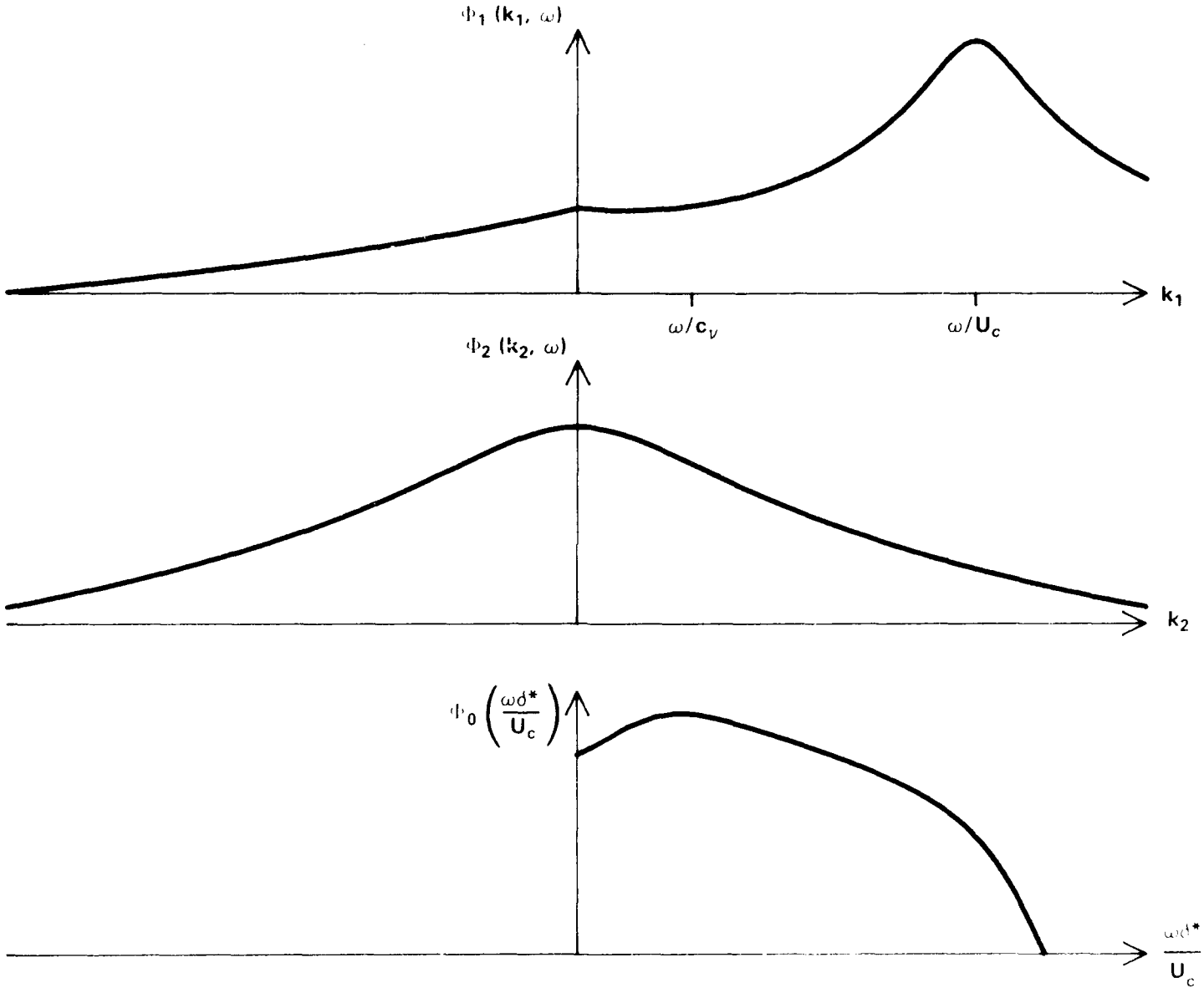

Figure 3 - Spectral Density Relationships

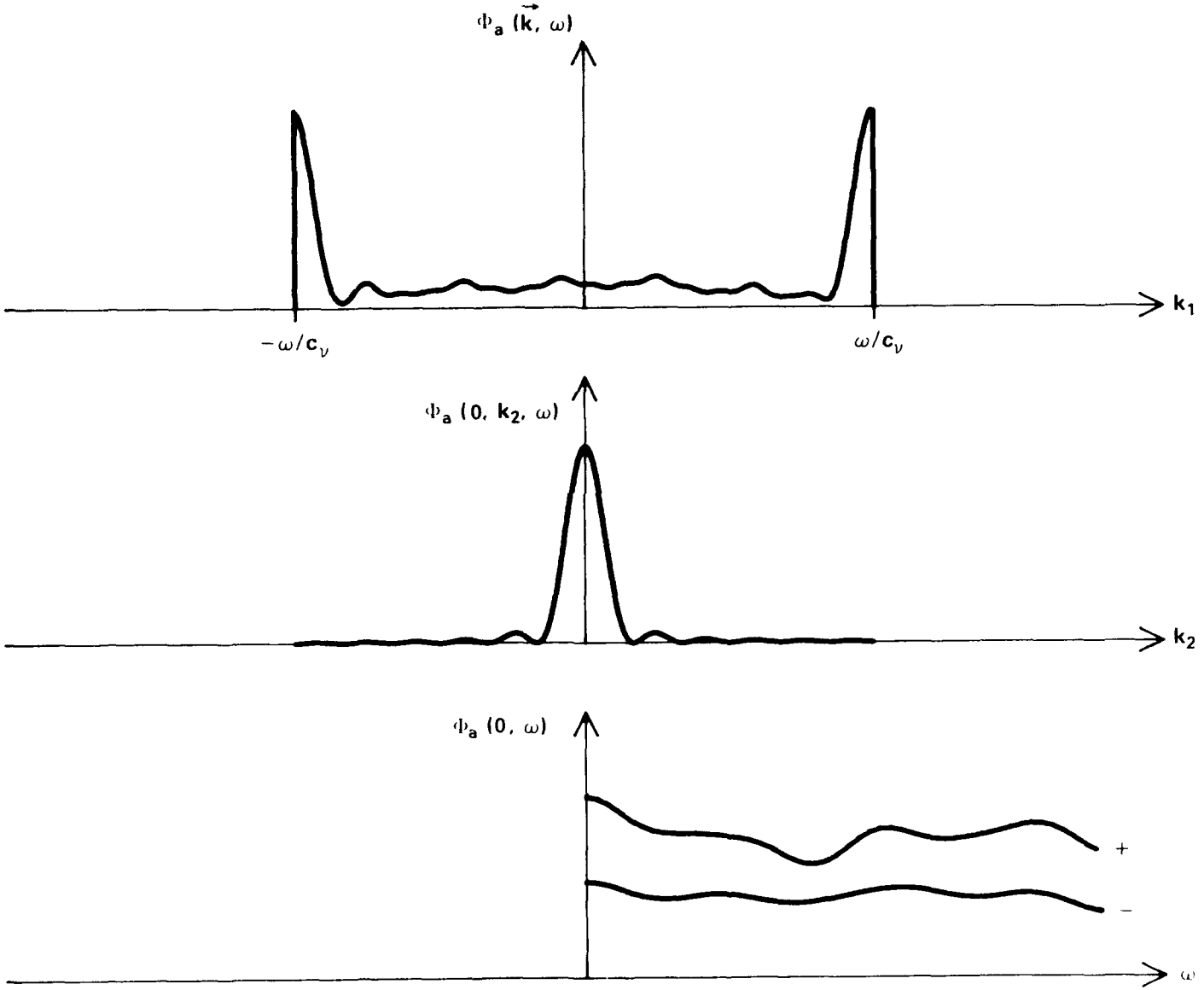

Figure 4 - Grazing Acoustic Pressure Fields

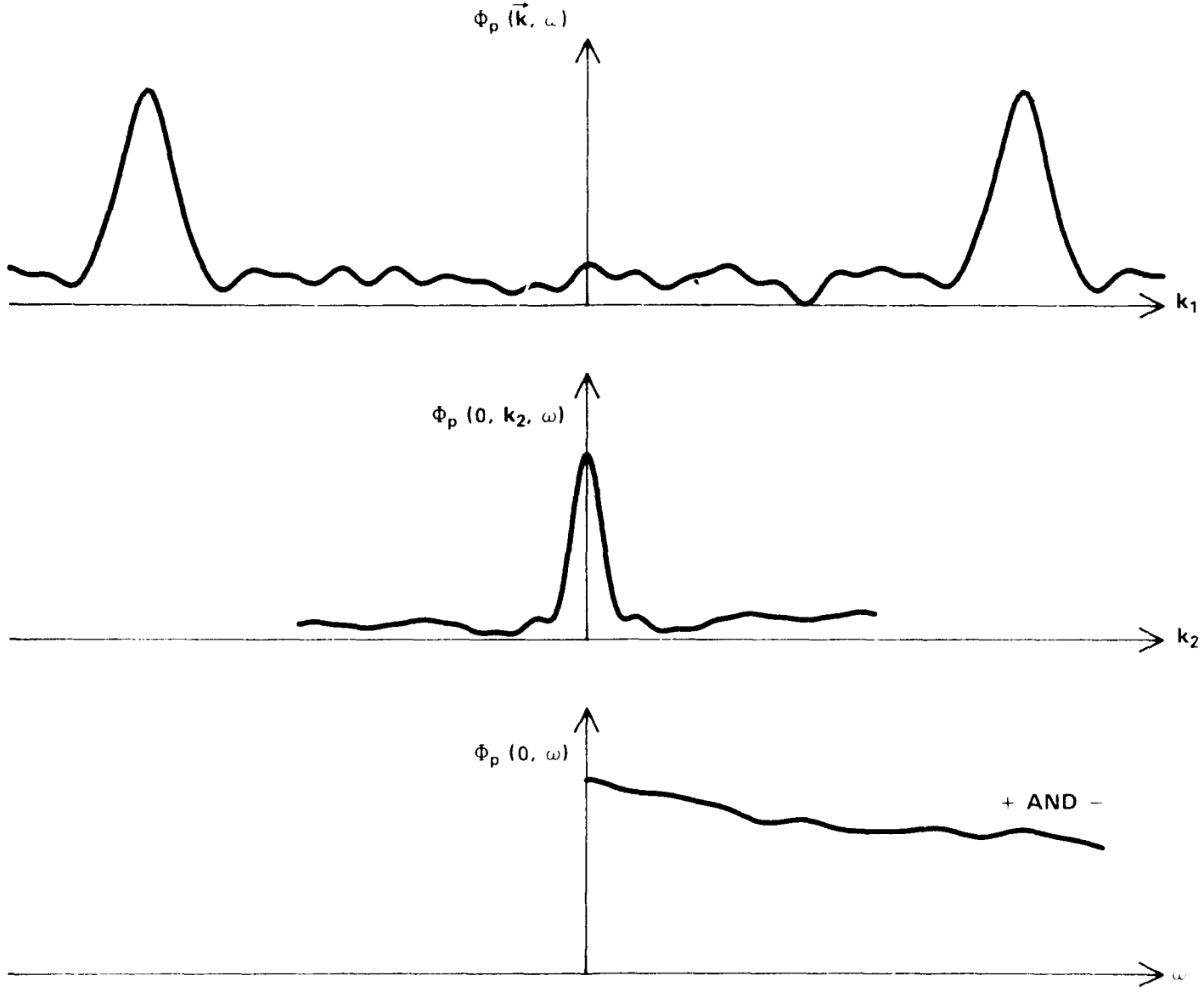

Figure 5 - Resonance Vibrational Pressure Fields

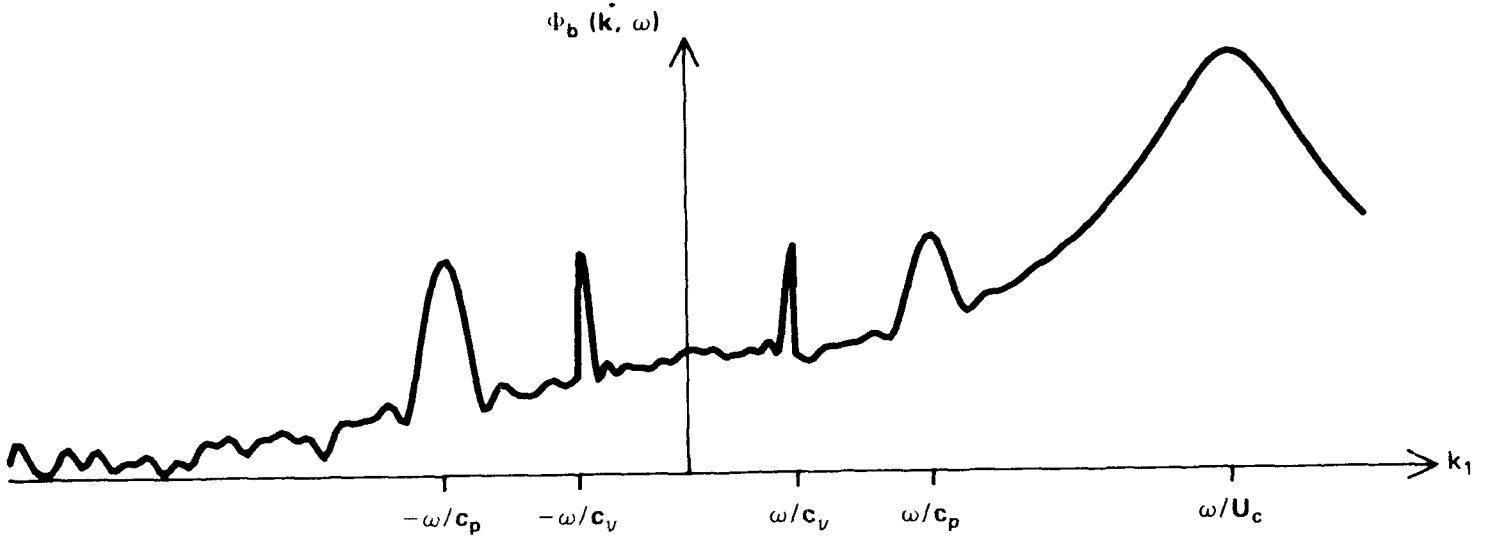

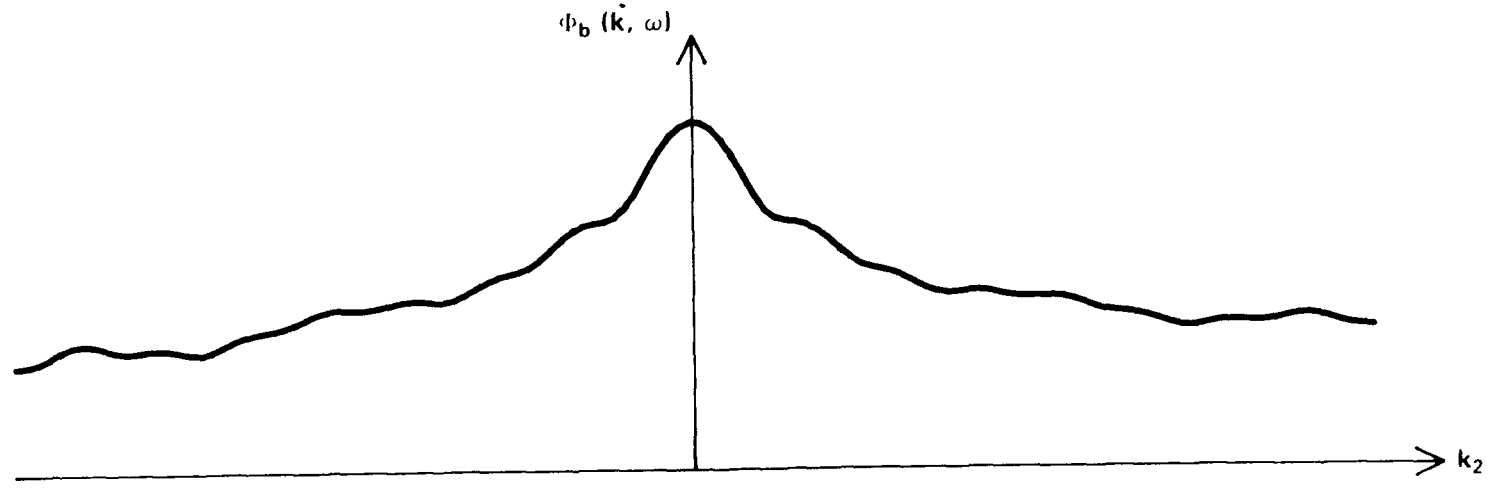

Figure 6 - Pressure Field on Boundary

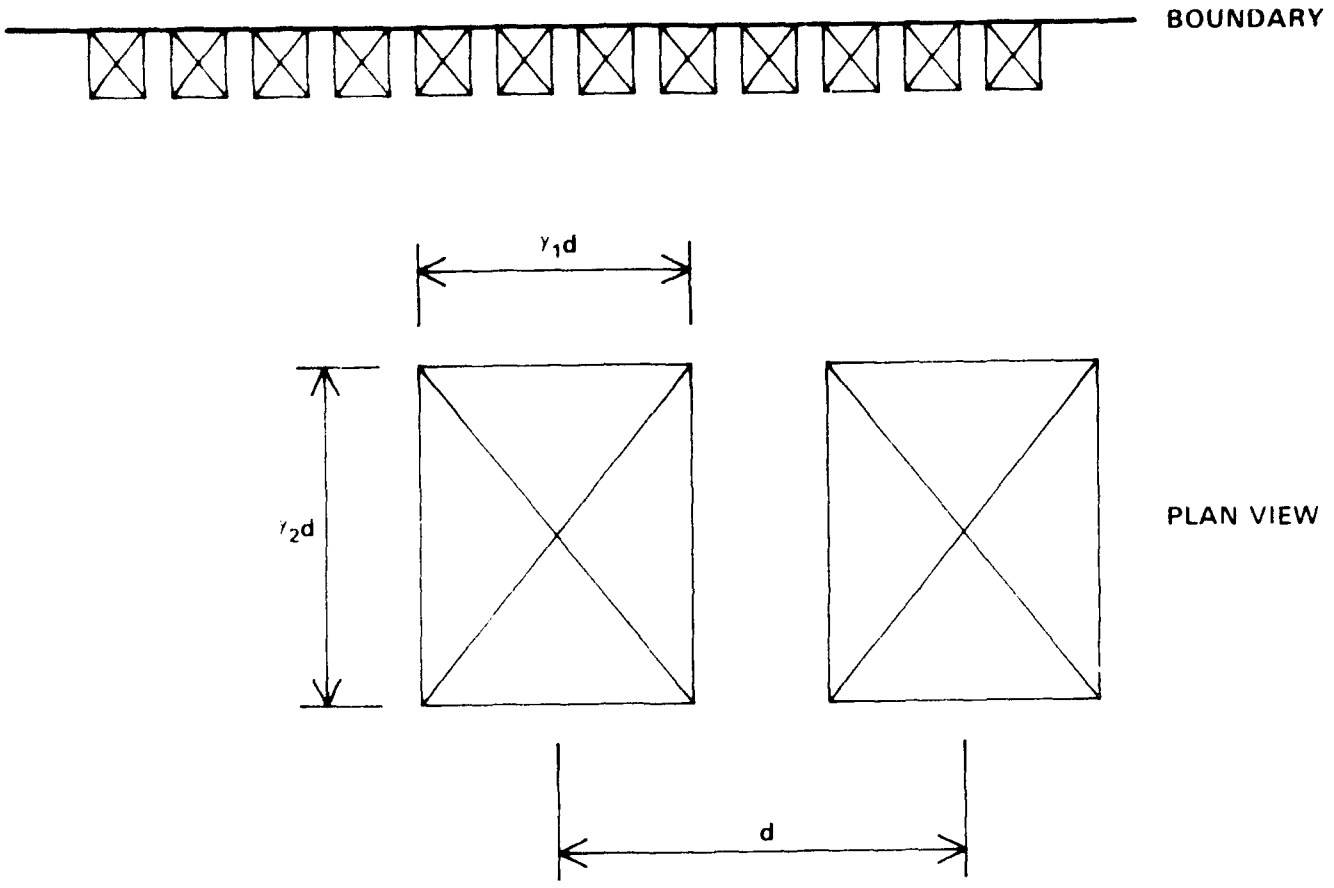

Figure 7 - Transducer System

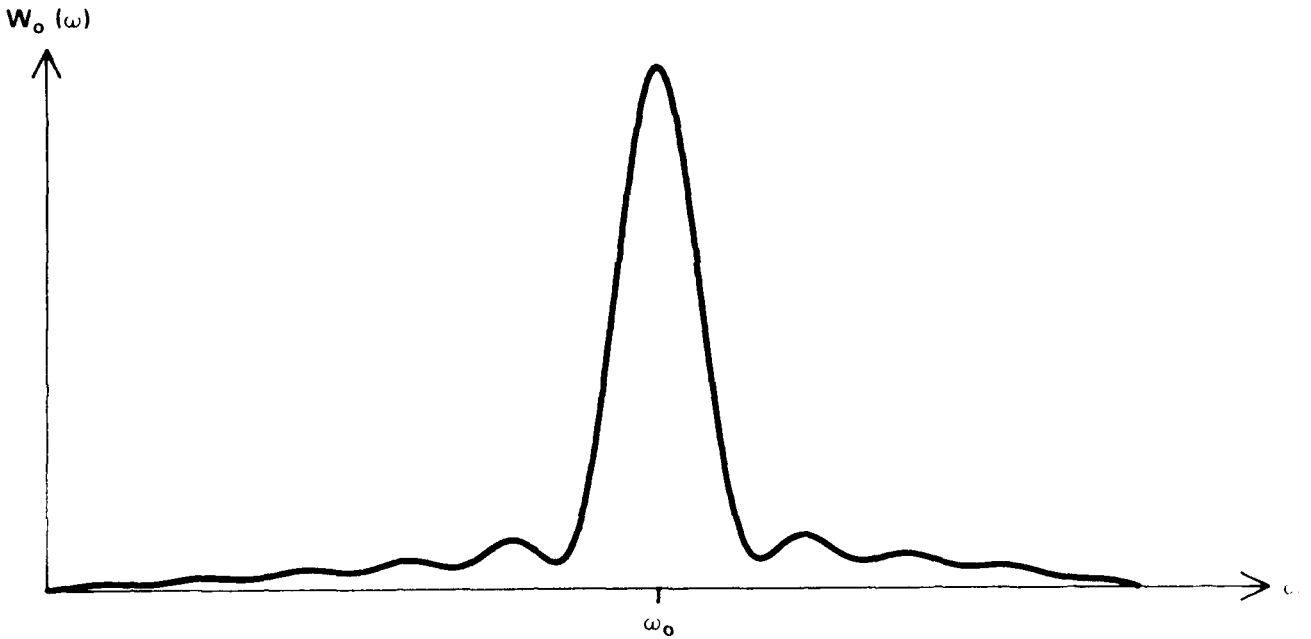

Figure 8 - Frequency Filtering Action

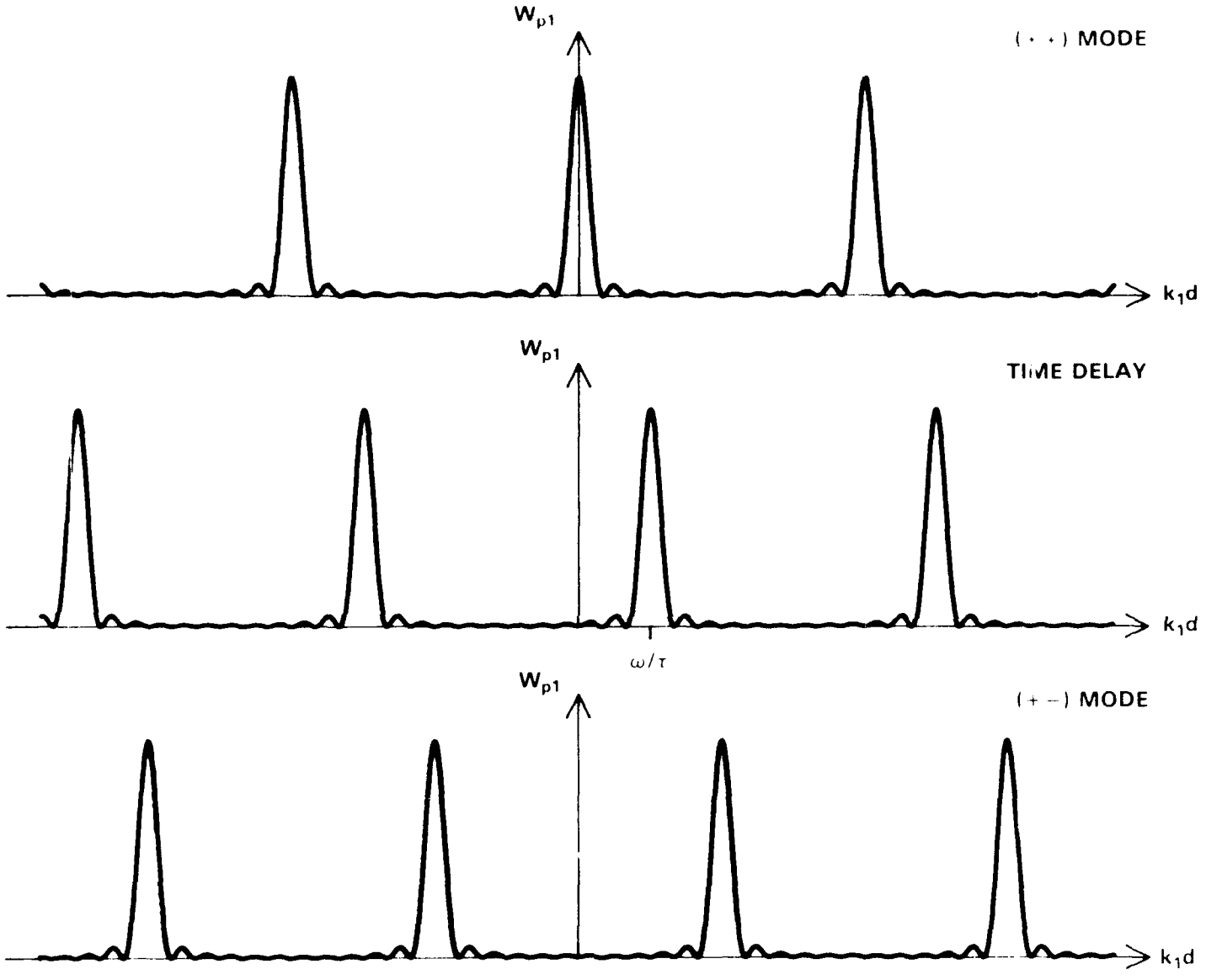

Figure 9 - Filtering Action of an Array of Point Transducers

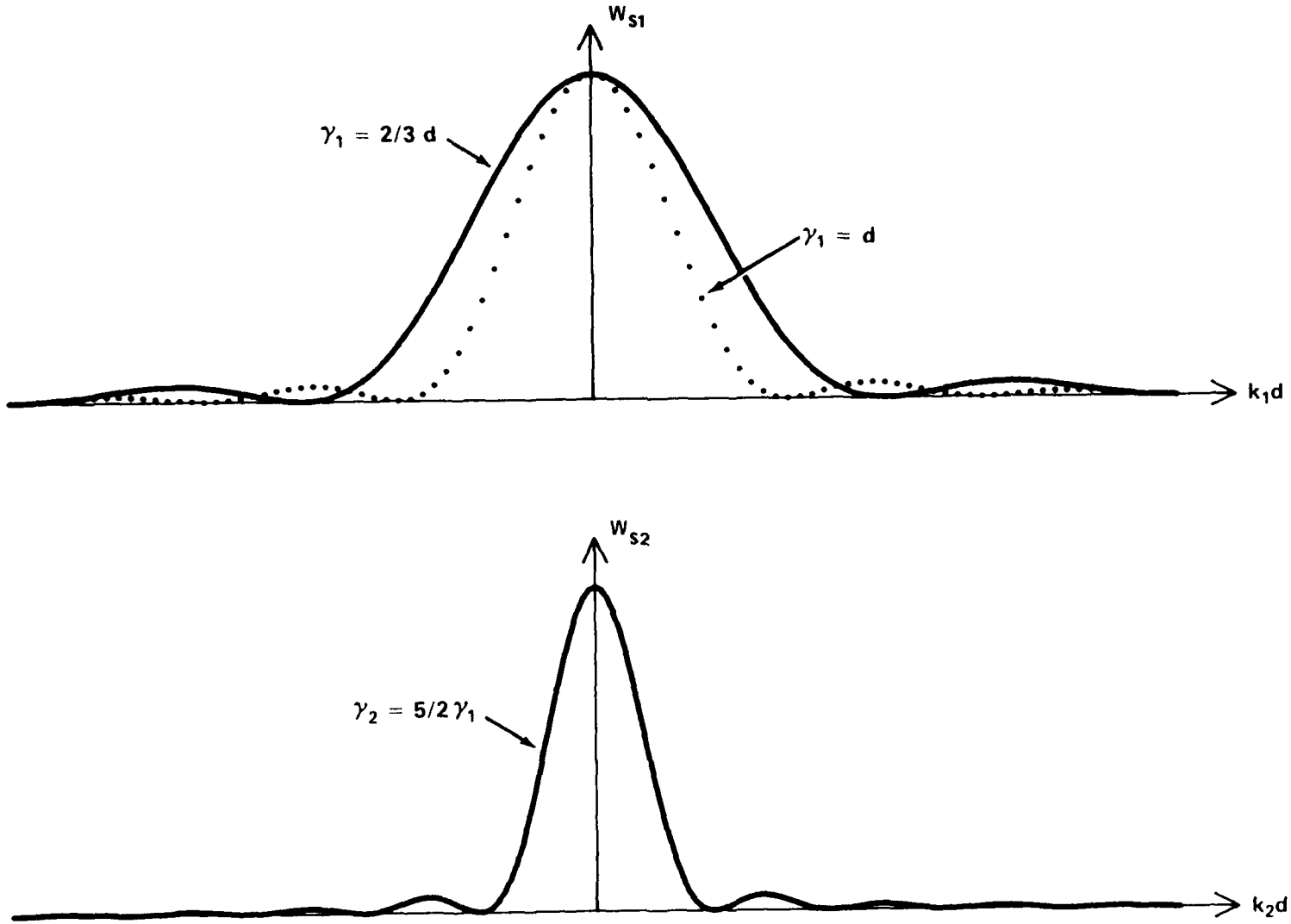

Figure 10 - Filtering Action of a Rectangular Transducer

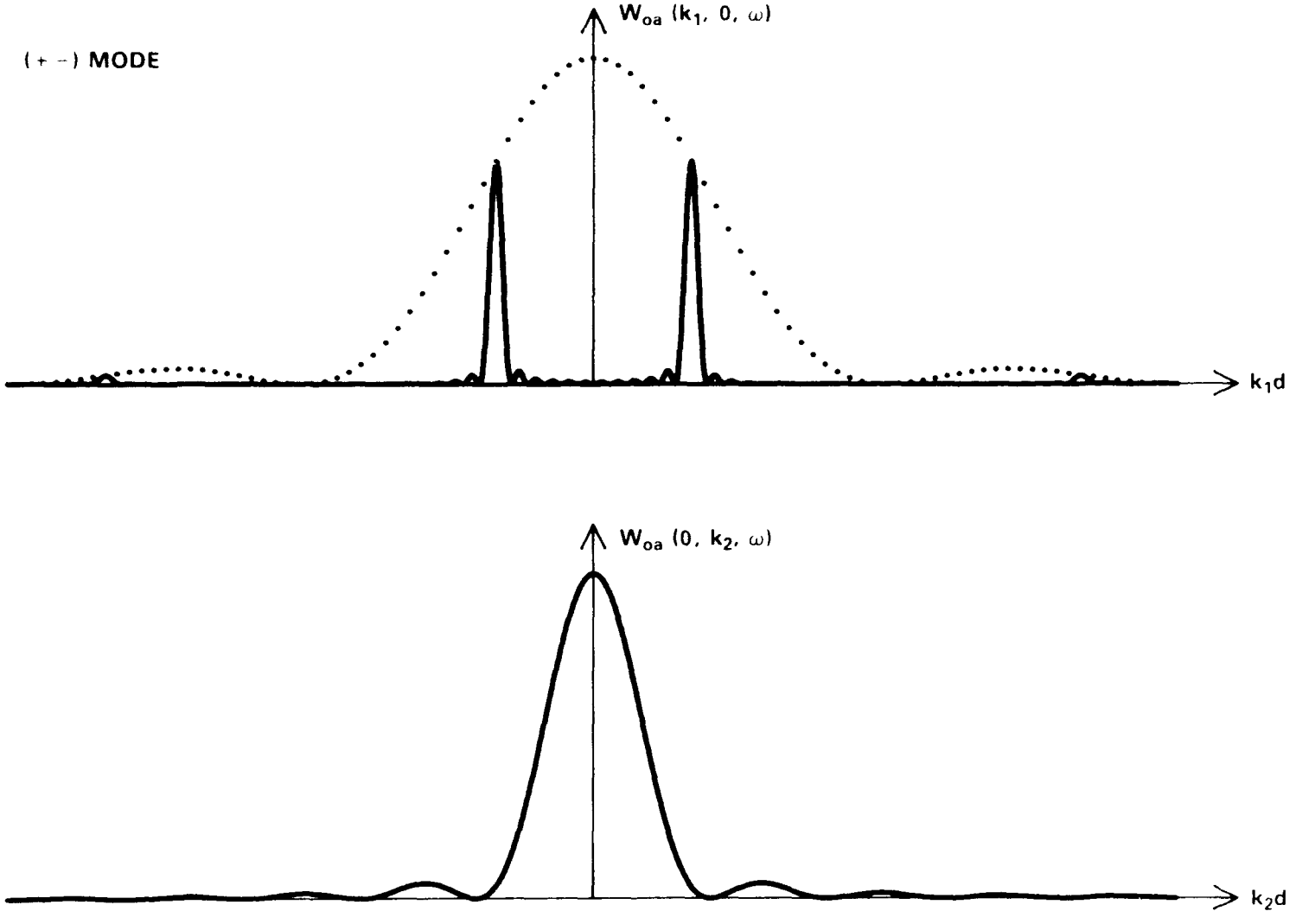

Figure 11 - Filtering Action of an Array of Rectangular Transducers

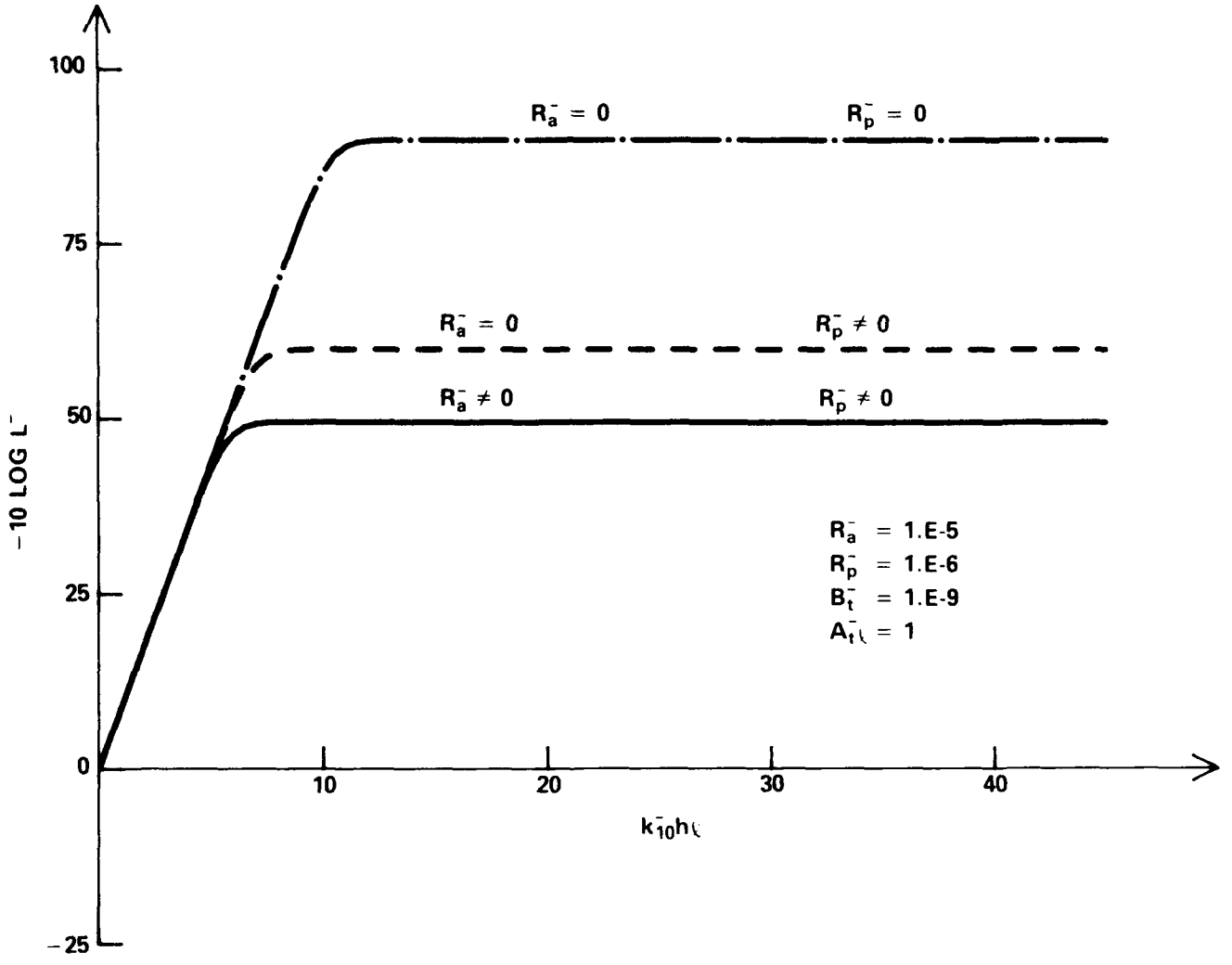

Figure 12a - Blanket Modification Factor for (+ -) Mode of Array

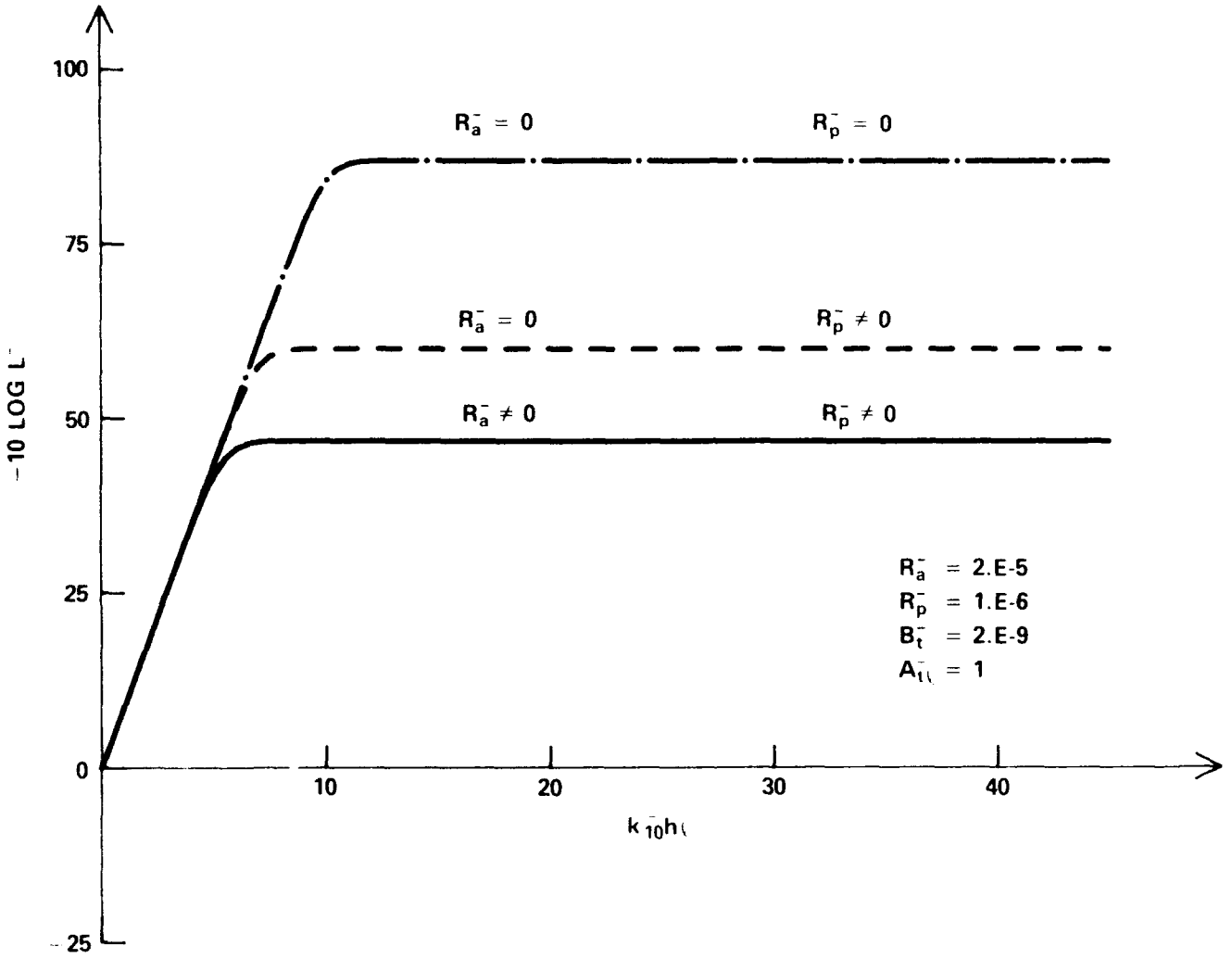

Figure 12b - Blanket Modification Factor for (+ -) Mode of Array

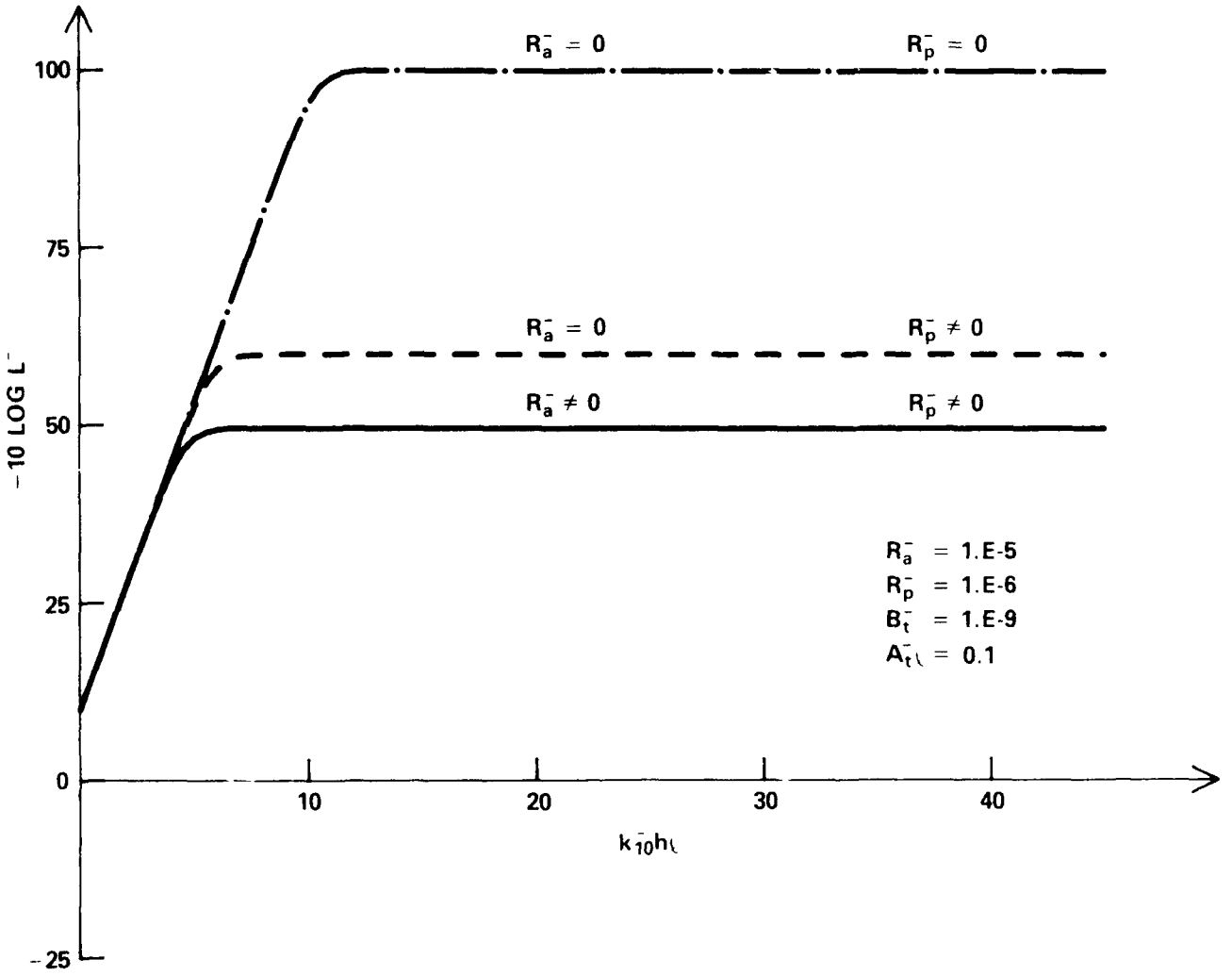

Figure 12c - Blanket Modification Factor for (+ -) Mode of Array

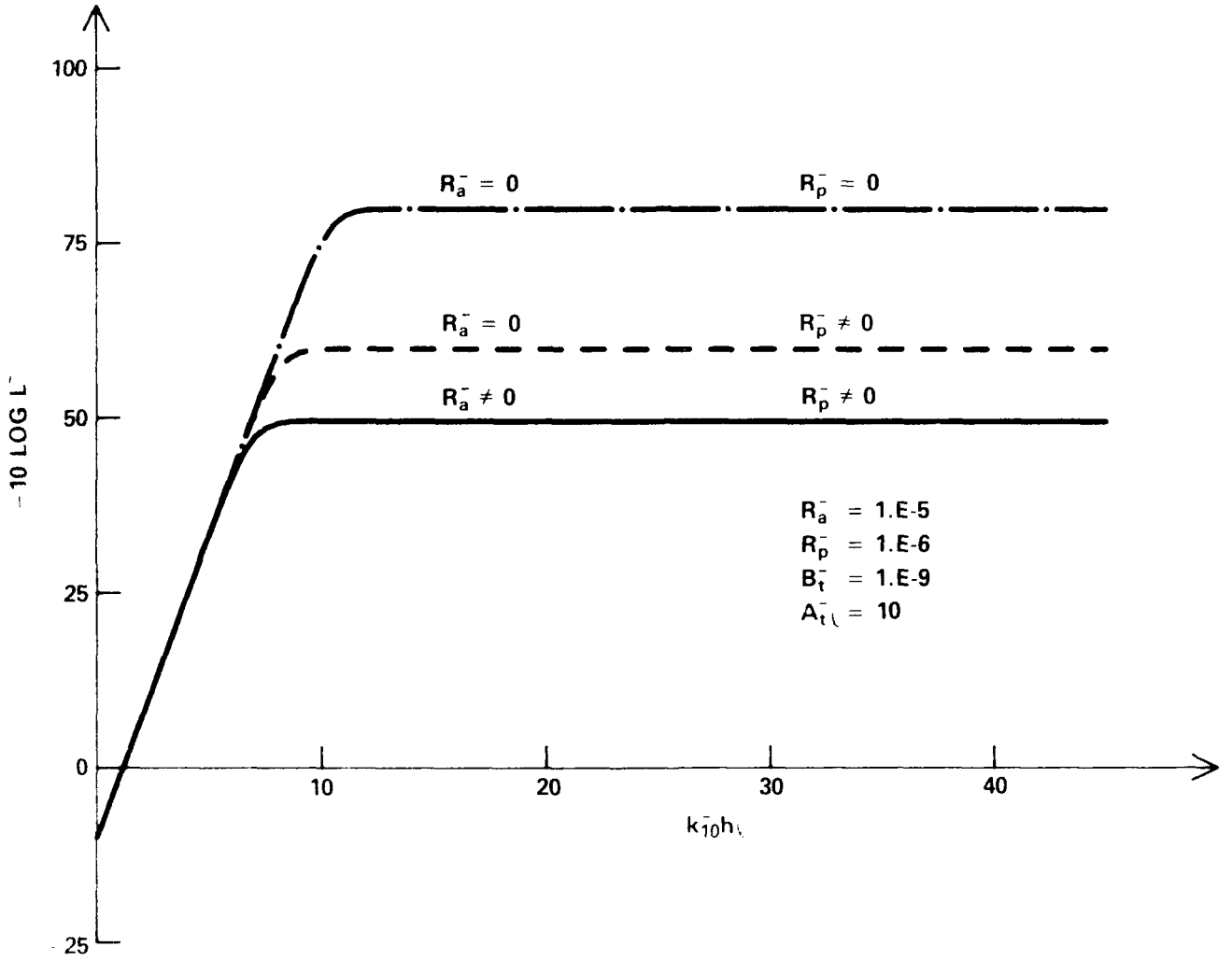

Figure 12d - Blanket Modification Factor for (+ -) Mode of Array

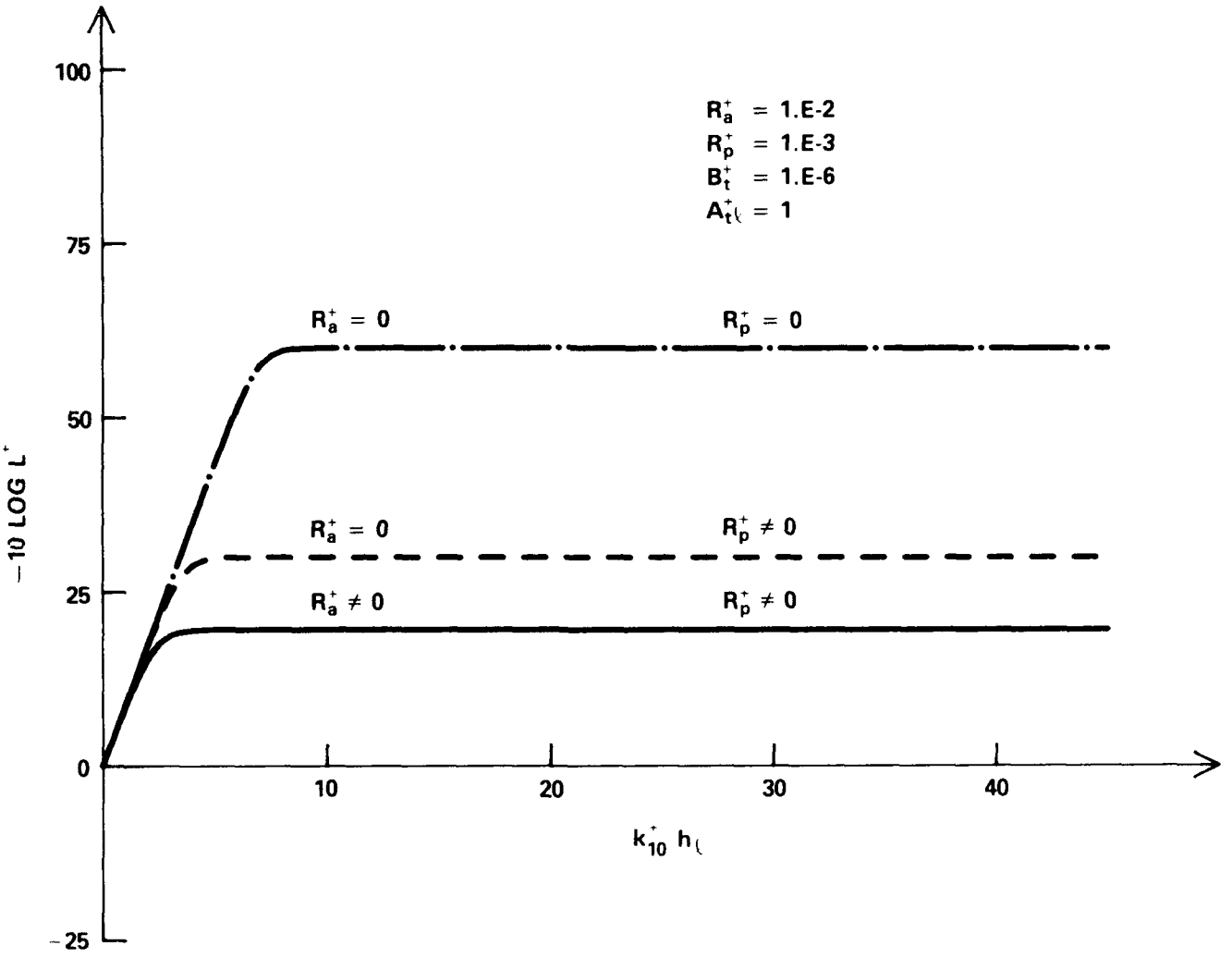

Figure 13a - Blanket Modification Factor for (++) Mode of Array

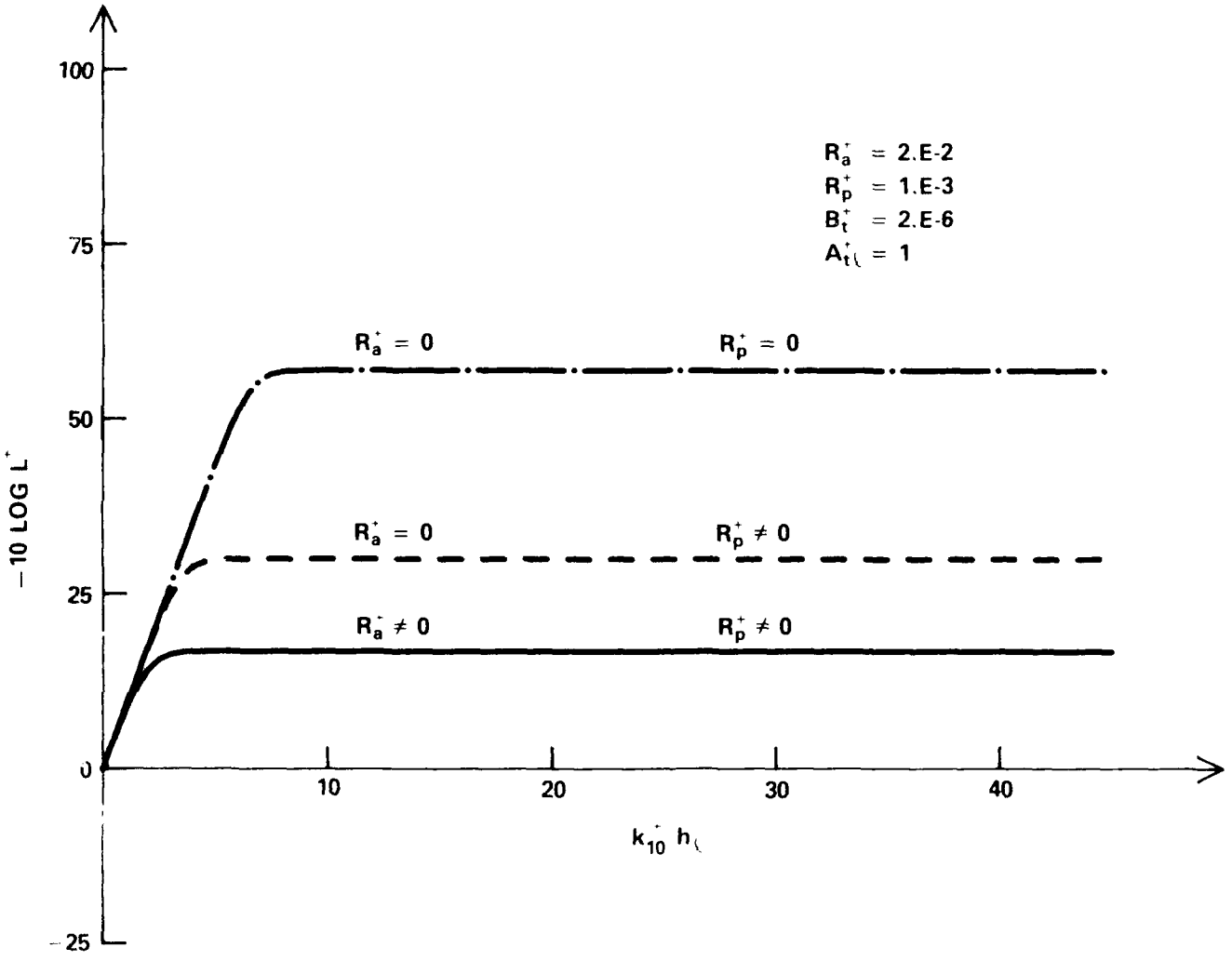

Figure 13b - Blanket Modification Factor for (++) Mode of Array

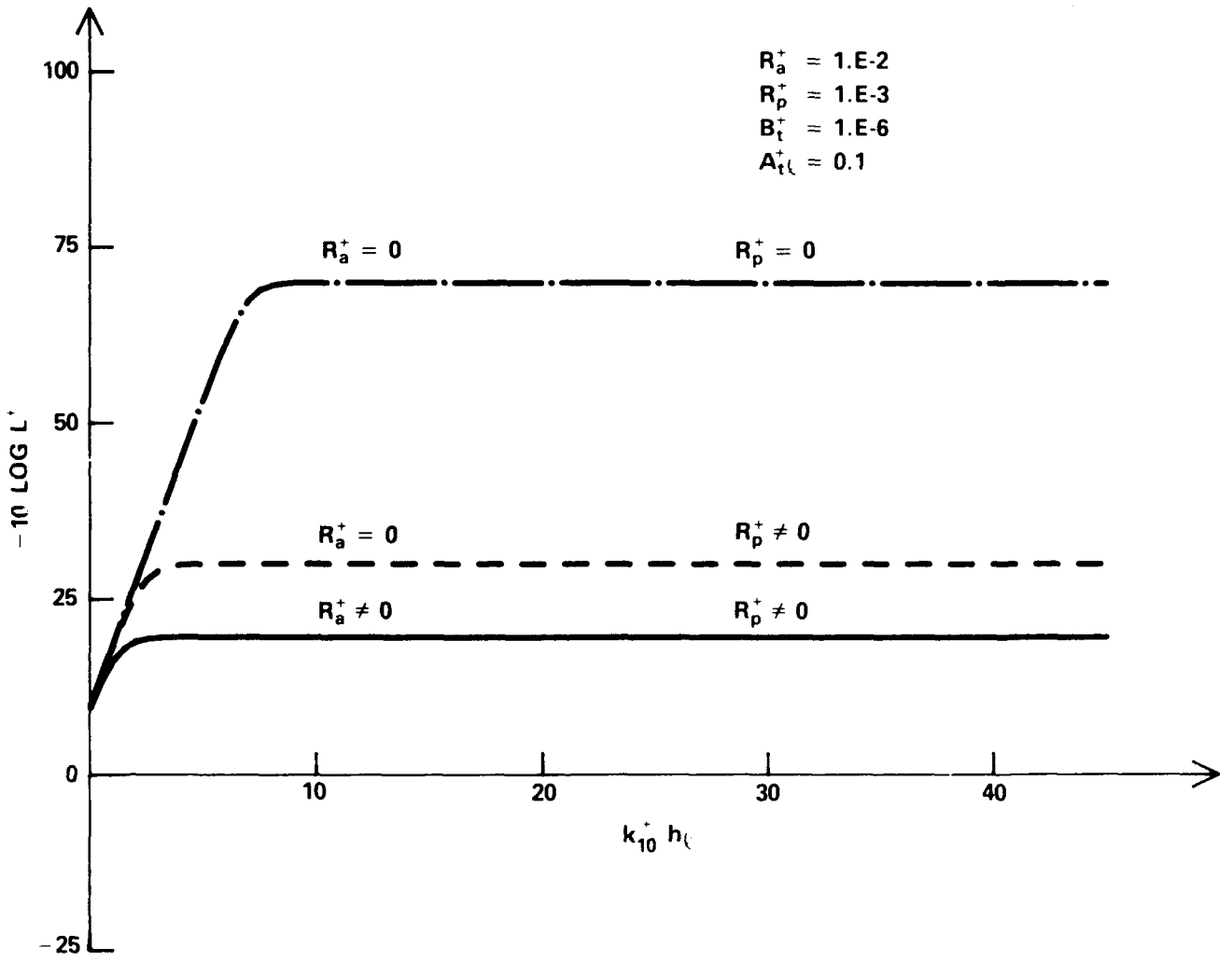

Figure 13c - Blanket Modification Factor for (++) Mode of Array

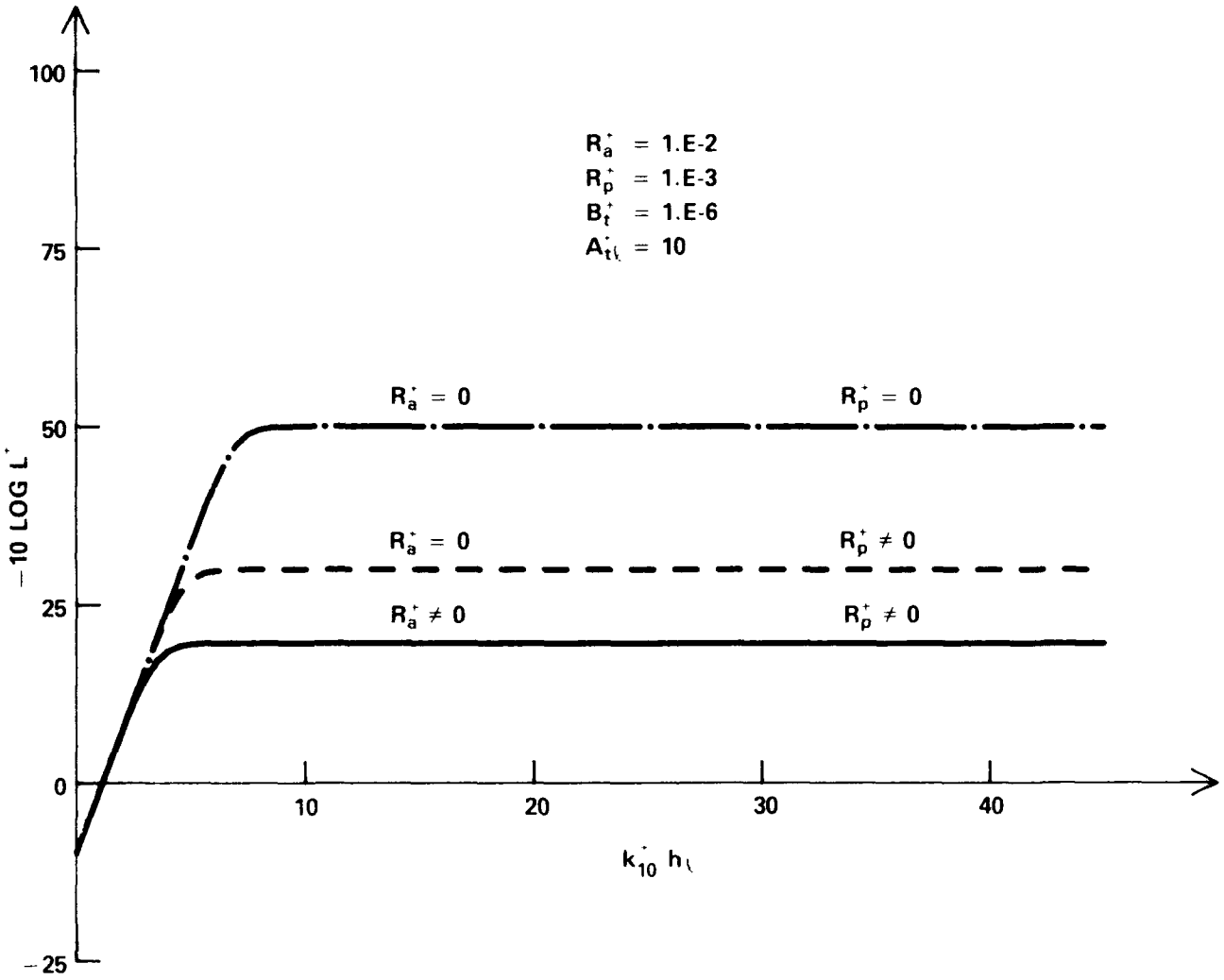

Figure 13d - Blanket Modification Factor for (++) Mode of Array

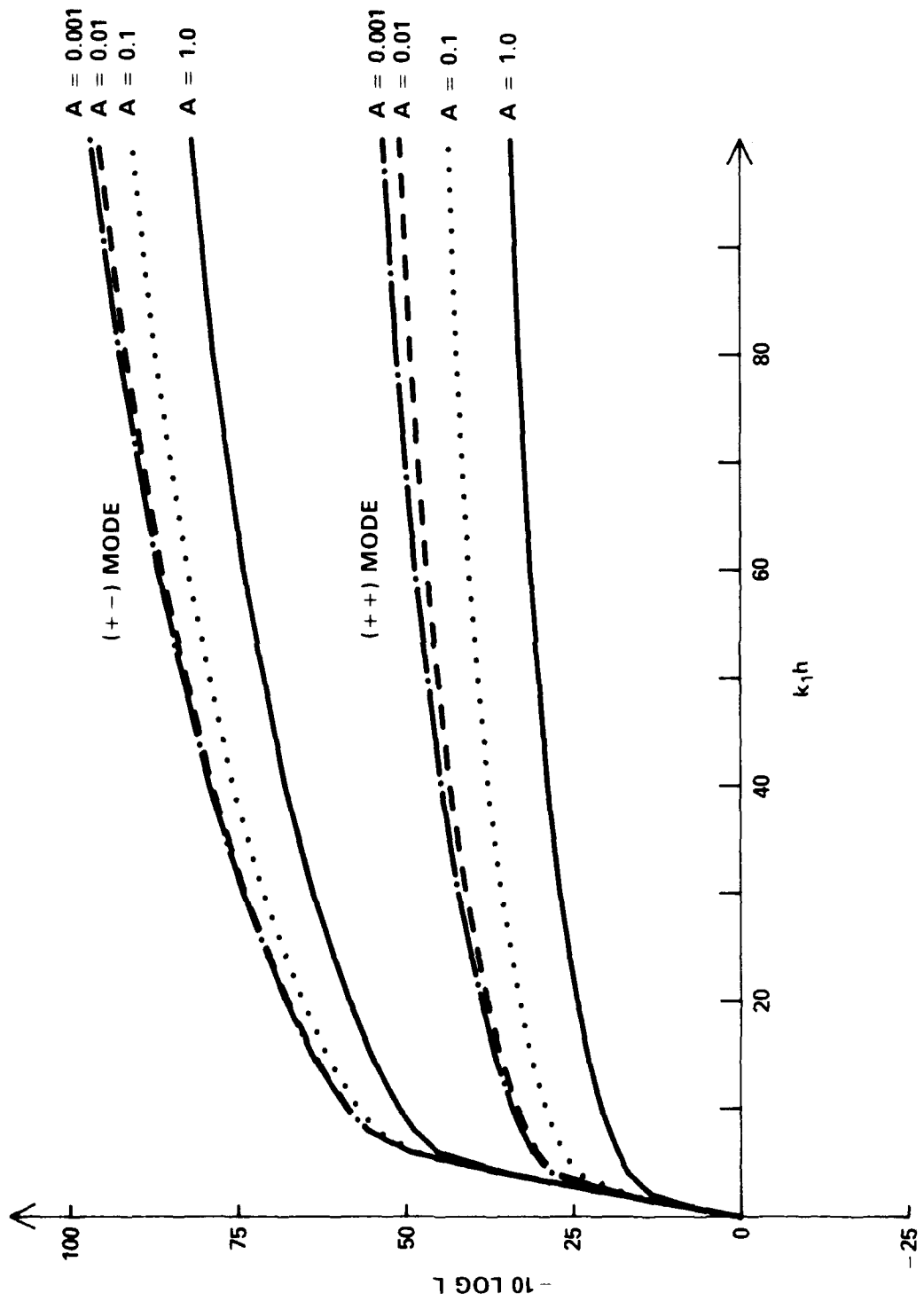

Figure 14 - Evaluation of the Wavevector Effectiveness Factor $\bar{C}_{t\ell}$

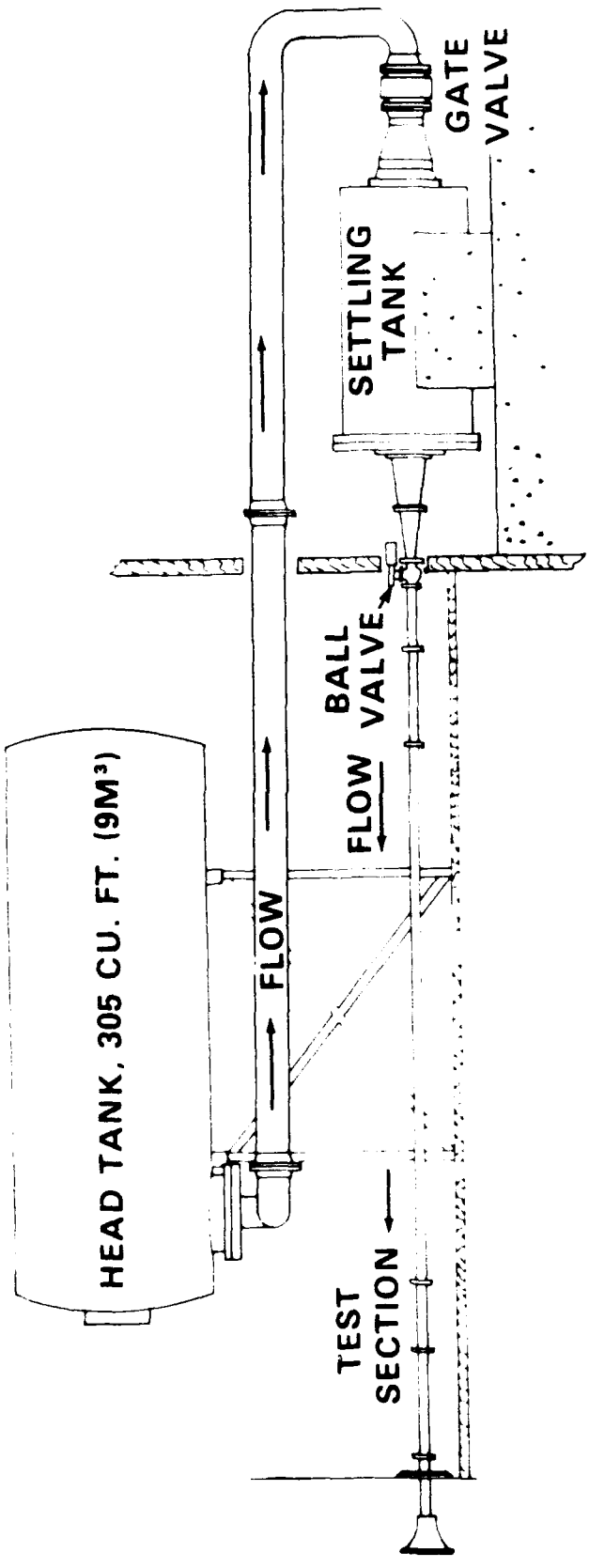

Figure 15 - Schematic of Quiet Pipe Flow Facility

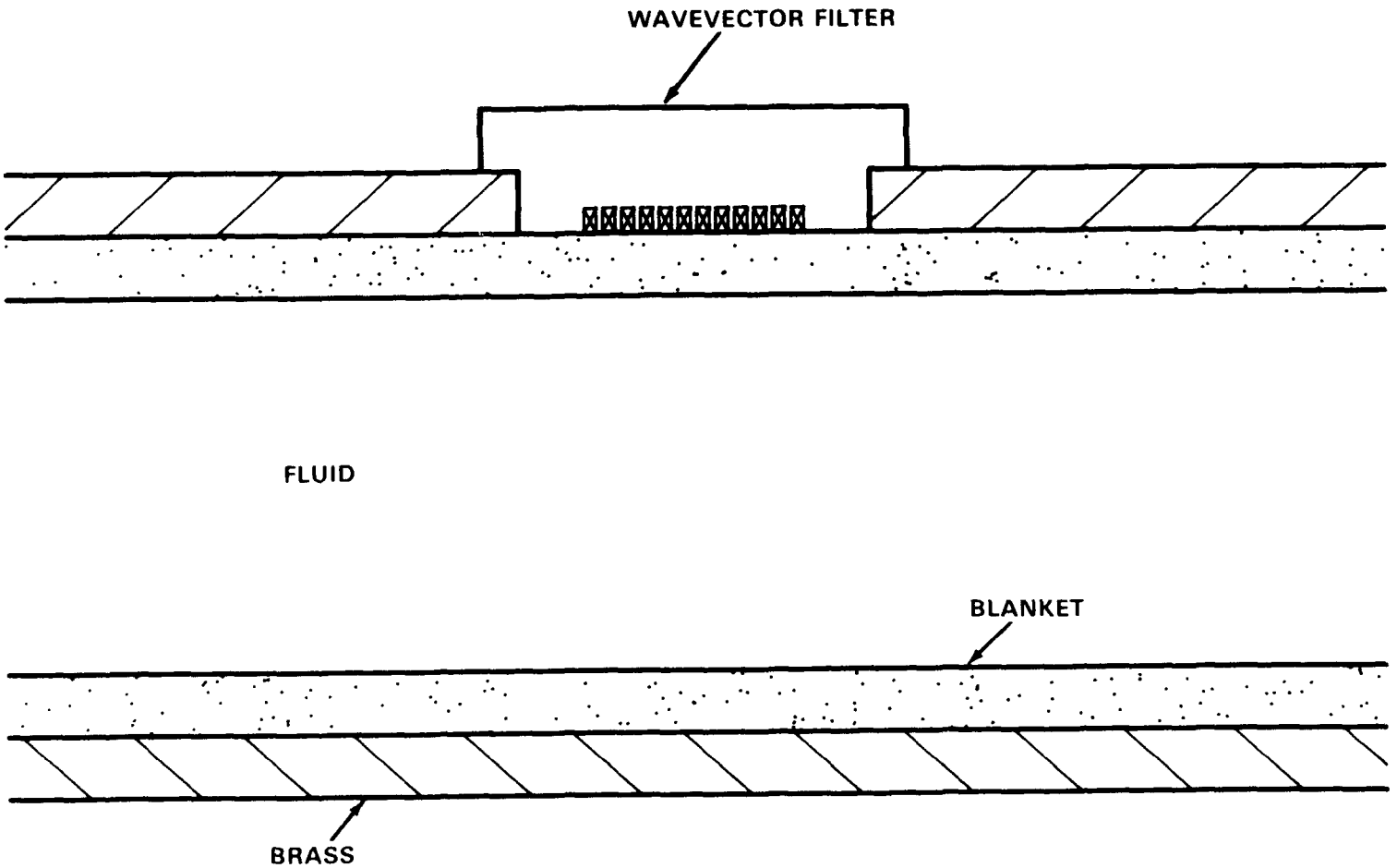

Figure 16 - Schematic of Test Section

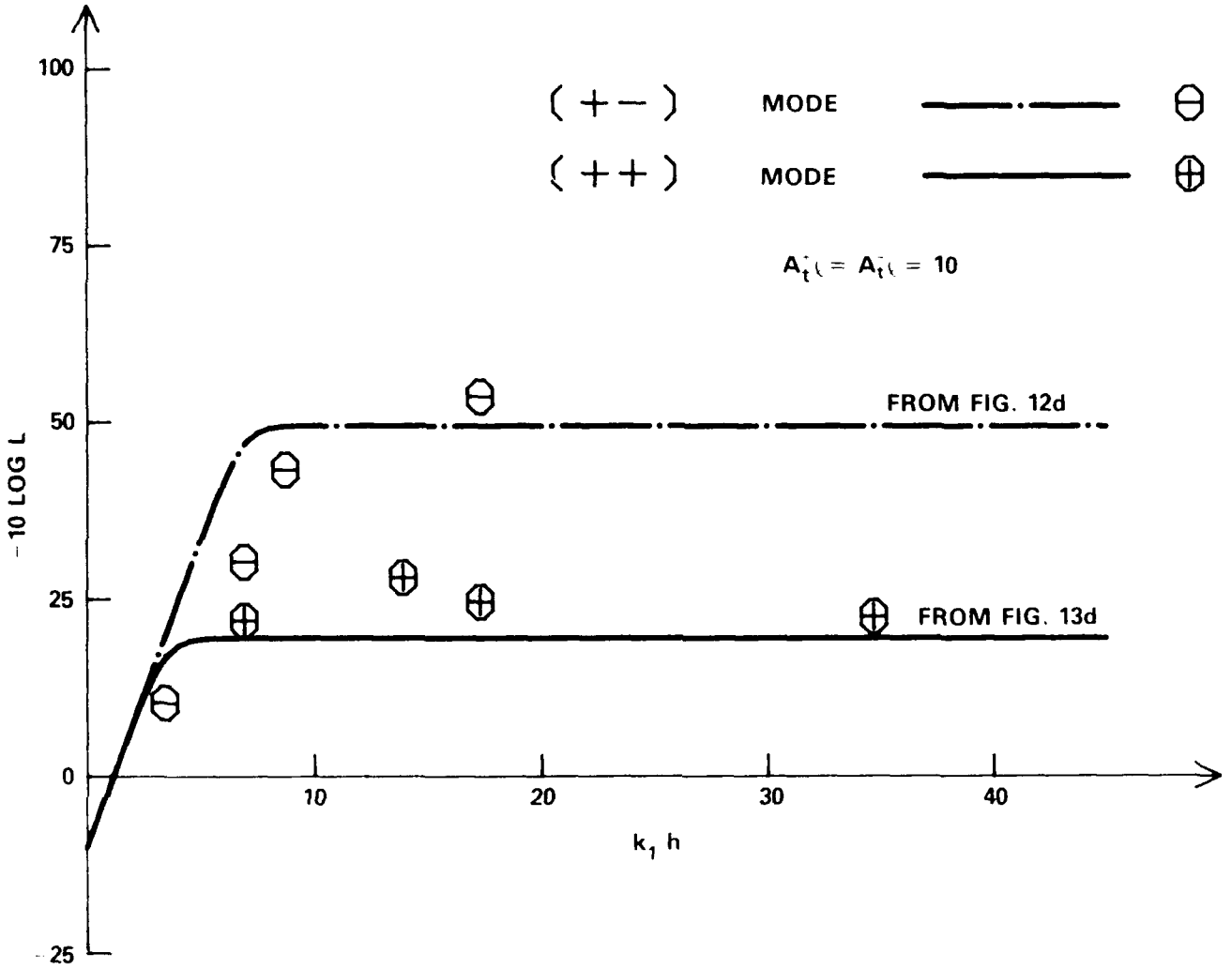

Figure 17 - Measured Wavevector Modification Factor I.

REFERENCES

1. Maidanik, G., "Flush-Mounted Pressure Transducer System as Spatial and Spectral Filters," Journal of Acoustical Society of America, 42, 1017-1024 (1967).

2. Maidanik, G. and A.J. Tucker, "Acoustical Properties of Coated Panels Immersed in Fluid Media," Journal of Sound and Vibration, 34(4), 519-550 (1974).

3. Maga, L.J. and G. Maidanik, "Response of Multiple Coupled Dynamic Systems," Journal of Sound and Vibration, 88(4), 473-488 (1983).

4. Maidanik, G., "Influence of Deviations and Variations in Transducers on the Filtering Actions of Spectral Filters," Journal of Acoustical Society of America, 55, No. 1, 170-183 (1974).

5. Maidanik, G. and T. Eisler, "Reasons and Means for Measuring the Spectral Density of the Pressure in a Subsonic Turbulent Boundary Layer," Journal of Sound and Vibration, 84(3), 397-416 (1982).

6. Hardy, G.H., A Course of Pure Mathematics, Cambridge University Press (1948).

7. Maidanik, G., "Surface Impedance Nonuniformities as Wave-Vector Convertors," Journal of the Acoustical Society of America, 46, 1062-1073 (1969).

INITIAL DISTRIBUTION

Copies	
1	DARPA
2	CHONR
	1 ONR 280
	1 Technical Library
2	NRL
	1 Code 5244/R.J. Hansen
	1 Technical Library
2	CHNAVMAT
	1 MAT 05
3	NAVSEA
	1 SEA 55N/S. Blazek
	1 SEA 55N2/A. Paladino
	1 Technical Library
6	NUSC/NLON
	1 Code 3292/C. Sherman
	1 Code 323/W. Strawderman
	1 Code 3233/R. Elswick
	1 Code 3233/S. Ko
	1 Code 3233/H. Schloemer
	1 Technical Library
1	NASA Langley/L. Maestrello
1	MIT/P. Leehey
1	U. of Michigan/W. Willmarth
1	N. Carolina State/T. Hodgson
1	ARL/Penn State/G. Lauchle
1	Bendix Corp/F. DeMetz
2	BBN
	1 N. Martin
	1 K. Chandiramani
1	CAA
1	Chase, Inc.
1	Poseidon Research

Copies	
1	Planning Systems, Inc.
1	ORI, Inc/R. Hoglund
1	Raytheon/S. Ehrlich
1	Wyle Labs/E. Stusnick

CENTER DISTRIBUTION

1	012.2	B. Nakonechny
2	012.3	D. Moran
1	1844	F. Henderson
1	19	M. Sevik
1	1901	M. Strasberg
10	1902	G. Maidanik
1	1905.1	W. Blake
1	1905.2	W. Reader
1	1905.4	D. Feit
1	193	J. O'Donnell
1	1932	W. Hoover
3	1933	S. Fisher R. Stefanowicz R. Wasserman
3	194	J. Shen M. Casarella K. Lewis
46	1942	F. Archibald L. Cole T. Farabee F.E. Geib (40 copies) M. Hayden Y. Hwang L. Maga
1	196	D. Vendittis
1	1965	M. Rumerman
1	522.1	Library
1	93	L. Marsh

DTNSRDC ISSUES THREE TYPES OF REPORTS

1. DTNSRDC REPORTS, A FORMAL SERIES, CONTAIN INFORMATION OF PERMANENT TECHNICAL VALUE. THEY CARRY A CONSECUTIVE NUMERICAL IDENTIFICATION REGARDLESS OF THEIR CLASSIFICATION OR THE ORIGINATING DEPARTMENT.

2. DEPARTMENTAL REPORTS, A SEMIFORMAL SERIES, CONTAIN INFORMATION OF A PRELIMINARY, TEMPORAPY, OR PROPRIETARY NATURE OR OF LIMITED INTEREST OR SIGNIFICANCE. THEY CARRY A DEPARTMENTAL ALPHANUMERICAL IDENTIFICATION.

3. TECHNICAL MEMORANDA, AN INFORMAL SERIES, CONTAIN TECHNICAL DOCUMENTATION OF LIMITED USE AND INTEREST. THEY ARE PRIMARILY WORKING PAPERS INTENDED FOR INTERNAL USE. THEY CARRY AN IDENTIFYING NUMBER WHICH INDICATES THEIR TYPE AND THE NUMERICAL CODE OF THE ORIGINATING DEPARTMENT. ANY DISTRIBUTION OUTSIDE DTNSRDC MUST BE APPROVED BY THE HEAD OF THE ORIGINATING DEPARTMENT ON A CASE-BY-CASE BASIS.